Winter 1-1-2012

The Establishment and Regulation of Melanocyte Stem Cells in Zebrafish

Thomas O'Reilly-Pol
Washington University in St. Louis

WASHINGTON UNIVERSITY IN ST. LOUIS

Division of Biology and Biomedical Sciences

Molecular Genetics and Genomics

Dissertation Examination Committee:
Stephen Johnson, Chair
Joseph Dougherty
Christina Gurnett
Craig Micchelli
Jason Mills
Jim Skeath

The Establishment and Regulation of Melanocyte Stem Cells in Zebrafish

By

Thomas Francis O'Reilly-Pol

A dissertation presented to the
Graduate School of Arts and Sciences
of Washington University in
partial fulfillment of the
requirements for the degree
of Doctor of Philosophy

December 2012

St. Louis, Missouri

TABLE OF CONTENTS

LIST OF FIGURES AND TABLES

ACKNOWLEDGEMENTS

I would like to thank the people that have helped shape the scientist that I have grown into. The person most responsible for this is undoubtedly my mentor, Steve Johnson. Without his support and encouragement, my views on science would not be what they are today.

Additionally, I owe a huge debt to the past and present members of the Johnson Lab, especially Shu Tu, Rob Tryon, Keith Hultman, Scott Higdon, Chao Yang, Ryan McAdow, Tim Chen, Anna Hindes, Melissa Wools, Kris Chain, Corey Johnson, Brian Stevens, Mike Foster, Erik Sanders and many others. They provided a collegial atmosphere for discussing problems and learning techniques.

ABSTRACT OF THE DISSERTATION

The Establishment and Regulation of Melanocyte Stem Cells in Zebrafish

By

Thomas O'Reilly-Pol

Doctor of Philosophy in Molecular Genetics and Genomics

Washington University Division of Biology and Biomedical Sciences, 2012

Dr. Stephen L. Johnson, Chairperson

Stem cells are the cells that regulate the growth and repair of tissues in adult organisms. In this thesis, I sought to develop methodologies to dissect the function and regulation of stem cells during zebrafish melanocyte regeneration.

In the first part of this thesis, I develop a drug based method of ablating melanocytes in the adult zebrafish body. The drug is a copper chelator, neocuproine (NCP) that I show causes death specifically of melanocytes in adult, which allows for regeneration from melanocyte stem cells (MSCs).

In the next part of the thesis, I employ clonal lineage statistical analyses to study the establishment, recruitment, and proliferation, differentiation, and survival of MSC daughter cells during larval melanocyte regeneration. These analyses suggest that MSCs are likely recruited at random for each regeneration event, and that approximately 84% of MSCs are recruited for any regeneration event. I demonstrate that *kit* signaling has a greater requirement during larval regeneration than during ontogeny and compare the regeneration of *kit* heterozygotes to wild type. The mutant heterozygotes have normal MSC recruitment and normal proliferation,

differentiation, and survival of daughter cells. The mutant has defective MSC establishment, with this defect being quantitatively sufficient to explain the regeneration defect observed. I then used further clonal lineage analysis to suggest that reduction of *kit* signaling causes inappropriate differentiation of fated MSCs into ontogenetic melanocytes. These analyses are not unique for comparison of *kit* mutants to wild type, so can easily be applied to dissect any gene or drug which affects regeneration.

In the final part of the thesis, I explore how many spermatagonia form the adult zebrafish male germline. An understanding of this number allows for efficient mutant screens, an essential part of the genetic dissection of any process. The zebrafish has approximately 485 spermatagonia, giving each male approximately 970 genomes which can be mutagenized. This number can be considered during mutant screen designs to eliminate redundant screening.

Chapter 1

Introduction

Updated from

Thomas O'Reilly-Pol and Stephen L. Johnson (2009)

"Melanocyte regeneration reveals mechanisms of adult stem cell regulation"

Seminars in Cell and Developmental Biology 5(4): 257-264

In developmental biology, we tend to use the term stem cell to describe cells with one or both of two features; the ability to produce multiple types of daughter cells (pluripotentiality), and the property of self renewal. For instance, the inner cell mass (ICM) of the blastula is a stem cell population for generating the diverse cell types of the embryo. These cells likely do not self renew during embryogenesis, but instead are consumed by the act of development. ICM cells can be coaxed to self renew in the petri-dish, an achievement that results in the laboratory embryonic stem cell (Martin, 1981). In contrast, cells of the skin, gut epithelium, and blood, tissues that are constantly turned over (physiological regeneration), are maintained by stem cells with limited potential to produce other cell types, but sufficient powers of self-renewal to maintain their target tissues through many decades of turnover. The different stem cells that maintain specific cells or tissues are collectively called adult stem cells. One such adult stem cell is the melanocyte stem cell (MSC). The existence of the MSC can be inferred from physiological regeneration of the mammalian hair follicle. At the end of each hair follicle cycle, matrix keratinocytes and the melanocytes that donate pigment to keratinocytes of the growing hair are shed, suggesting adult stem cell are responsible for generating both new keratinocytes and new melanocytes for the next hair follicle cycle (Oshima et al., 2001). Use of the dct:lacZ transgenic mouse (Mackenzie et al., 1997) together with BrdU incorporation studies provided direct evidence of the MSC in the bulge region of the mammalian hair follicle (Nishimura et al., 2002). A variety of human depigmenting syndromes, including vitiligo and age-associated graying, are the result of loss of MSCs from the hair follicle (Nishimura et al., 2005).

The goal of studying melanocyte regeneration in zebrafish is to understand the mechanisms underlying regulation of adult stem cells in general, or melanocyte stem cells in particular. More and more evidence is accumulating for the existence of a variety of different

adult stem cells in mammals, but the nature of the mechanisms that regulate them, and can then be exploited to regenerate tissues for therapeutic purposes lags behind. The hope is that simple paradigms for ablating melanocytes and then challenging their ability to regenerate in zebrafish will lead to the identification of mutations or of drugs that affect the regulation of the melanocyte stem cell, that can then translate into applications for manipulating a variety of stem cells in therapeutic applications. Outlined in Figure 1-1 are some of the mechanisms that can be expected to be involved in adult stem cell regulation, including the embryonic mechanisms that **establish** the stem cells, that **recruit** the stem cell to produce new cells in response to growth or injury, and then **differentiate** them. It also seems likely that the stem cells are **repressed** by intact target cells or tissues. Finally, stem cells **renew** themselves when they generate new cells for development. However, unlike in mouse (Nishimura et al., 2002), the zebrafish melanocyte stem cell (MSC) has not been directly identified, and the inferences that we draw about the zebrafish melanocyte stem cell come indirectly from the analysis of their differentiated daughters, the melanocytes, following regeneration or pigment pattern metamorphosis. Here, I discuss several examples of regenerating melanocytes that shed light on one or more of the mechanisms involved in adult stem cell regulation.

Two populations of melanocytes in the regenerating fin

Fin regeneration in zebrafish was first described by Goodrich and his colleagues (Goodrich and Nichols, 1931) in his studies to use re-establishment of pigment patterns in the regenerating fin to provide a different perspective on the mechanism responsible for the patterning of the melanocyte stripes. Those experiments are summarized in Figure 1-2. Briefly,

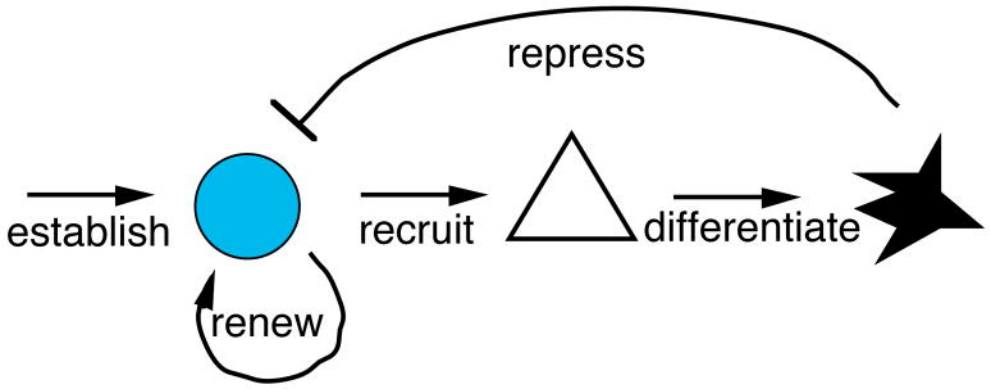

Figure 1-1. Mechanisms utilized in Melanocyte Stem Cell regulation. This schematic shows different types of mechanisms that are likely involved regulating MSCs during regeneration experiments. Blue circle represents the MSC, triangle represents melanoblast intermediate, and the black cell represents a mature melanocyte.

within 4 days after amputation (converted to standard regeneration stages at 25 degrees) melanocytes are observed scattered throughout the regenerate. By 7–8 days, most of the melanocytes in the proximal, or developmentally oldest part of the regenerate, are now arranged in distinct stripes, and scattered melanocytes outside the presumptive stripe are only found in the most distal, or developmentally youngest region of the regenerate. This pattern of melanocytes in the regenerating fin persists until several weeks after amputation, at which time regeneration is largely completed and no melanocytes are found in the distal, presumptive interstripe regions of the regenerate. These studies suggested that the distal, scattered melanocytes are also developmentally younger, and that maturation of the regenerate then leads melanocytes in interstripe regions to either die, or migrate into stripe regions. These studies of Goodrich, together with more modern tools and the availability of mutants that affect pigment pattern in zebrafish later led to the studies of Rawls and Johnson (Rawls and Johnson, 2000; Rawls and Johnson, 2001) to explore the origins and genetic control of development of melanocytes in the regenerating fin.

In principle, without evoking exotic models such as transdifferentiation or re-establishment of stem cells, regenerating melanocytes can come from one of two sources: cell division from existing, pigmented melanocytes, or recruitment of melanocyte precursors or stem cells to re-enter developmental pathways, reenter the cell cycle, and produce new melanocytes de novo. For instance, the first model, whereby differentiated cells re-enter the cell cycle and simply divide to grow new cells seems to be the case for regeneration of the bone or lepidotrichia in regenerating zebrafish fin, as revealed by BrdU incorporation or by lineage analysis of mosaic clones of transposons expressing GFP under strong ubiquitous promoters (H. Huang and S. Johnson, unpublished). In contrast, the second model seems to hold for hair cell regeneration in

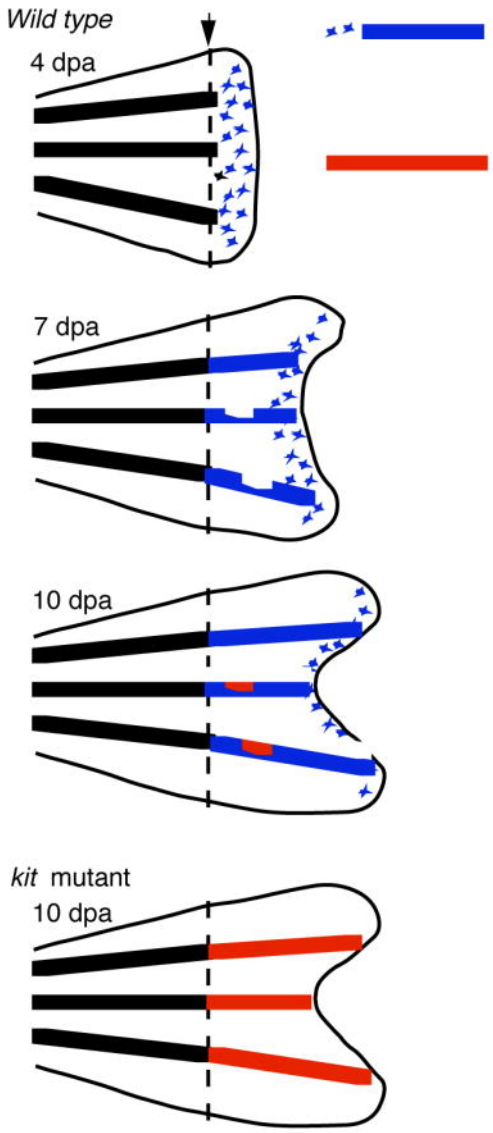

Figure1-2. Two types of melanocytes contribute to the regenerating stripe in the regenerating zebrafish caudal fin. Schematic shows that primary regeneration melanocytes (in blue) first develop in scattered locations in distal or developmentally youngest part of fin. Secondary, or regulatory melanocytes (in red), develop in more proximal or developmentally older parts of the regenerate, in response to deficits in the primary regeneration melanocyte stripe. In *kit* mutants, that lack primary regeneration melanocytes, secondary regulatory melanocytes account for the entire population of regeneration melanocytes.

he lateral line, whereby supporting glial cells, that seem to serve as the stem cell for the neuromast, divide to produce new hair cells following neomycin induced hair cell ablation (Ma et al., 2008).

Which of these models hold for melanocyte regeneration in the regenerating fin was solved by using the pre-existing melanin in differentiated melanocytes as a lineage marker, and preventing new melanin synthesis in any newly differentiated melanocytes by incubating fish in a melanin synthesis inhibitor, phenylthiourea (PTU). The finding that preexisting melanin is not partitioned to the vast majority of melanocytes that are found in the regenerating fin suggested that regeneration melanocytes develop de novo from undifferentiated precursors, rather than by division of differentiated, pigmented cells (Rawls and Johnson, 2000).

The existence of two distinct populations of regeneration melanocytes in the regenerating fin is suggested by the kinetics of melanocyte appearance in the *kit* mutant regenerates. In contrast to regeneration in the wild type fin, that produces de novo melanocytes throughout the regenerate beginning at 4 days, and then restricted to distal, developmentally younger tissue at 7 or 10 days following amputation, *kit* mutants have no new melanocytes in the regenerate at 4 or 7 days (Rawls and Johnson, 2001). However, by 8–10 days *kit* mutants begin to develop new melanocytes. In contrast to wild type fish that develop melanocytes throughout the distal, or youngest, area of the regenerate, melanocytes in the *kit* mutant first appear restricted to the presumptive stripe, in the developmentally oldest regions of the regenerate (Rawls and Johnson, 2001). This finding reveals that there are two distinct populations of melanocytes that contribute to regeneration. First, an early, primary population develops throughout the newest, or distal, portion of the regenerate. The development of this population is promoted by the *kit* receptor tyrosine kinase. Lacking *kit* function, a second, regulatory population of melanocytes develops.

This population appears after a delay of approximately 4 days, in the proximal or developmentally older part of the regenerate, and only in the presumptive stripe. This population plays little or no role in normal stripe regeneration, except perhaps to fill in gaps or holes left by the primary population. However, in the absence of the *kit*-dependent primary population, such as in *kit* mutants, the secondary or regulatory population generates as many melanocytes as does the wild-type regenerate (Rawls and Johnson, 2001).

In situ expression analysis revealed that *kit* transcript is upregulated in cells near the amputation plane as early as 1.5 days post amputation (dpa), suggesting an early role for kit in recruiting stem cells back into regeneration pathways (Rawls and Johnson, 2001). However, it remained possible that kit function was also required to establish these stem cells during embryonic development. To address this question, Rawls and Johnson (2001) isolated a temperature-sensitive allele of *kit* (Rawls and Johnson, 2001). Reciprocal shifts from embryonic stages through stages after amputation revealed that *kit* was not required for establishing the melanocyte stem cells during embryonic development, but rather was required beginning two days after amputation. Thus, the role for *kit* in fin melanocyte regeneration is not in establishing the stem cell population, but instead to recruit the stem cells back into development, or in some early stage of melanocyte differentiation (Rawls and Johnson, 2001).

The finding that fin melanocytes develop by two different pathways, one dependent on *kit* function, and a second regulatory pathway that produces melanocytes independent of *kit*, raises several important issues in adult stem cell regulation. One question is: how do stem cells know when they have generated sufficient cells to repair the missing tissue? The MSCs of the regenerating fin seems to have solved this problem by using two distinct mechanisms. First, dependent on *kit* function, the stem cells generate excess melanocytes that are distributed

throughout the distal, or developmentally youngest, part of the regenerate. Rather than responding to loss of repression from pre-existing melanocytes, the primary melanocytes seem to respond positively to a fin-wide regeneration signal, that then generates excess melanocytes, which are then pruned down to the numbers needed for the appropriate stripe. A compelling question is: what is the nature of this positive signal that recruits stem cells into the primary regeneration pathway, and is this the same signal used to evoke regeneration of other tissues in the regenerating fin?

In contrast to the primary, *kit*-dependent melanocytes, the second, *kit*-independent population of melanocytes seems exquisitely sensitive to the presence of melanocytes, and appears to generate new melanocytes only to fill in holes or gaps in the stripe pattern after the primary population has done its best. A question raised by these two different types of melanocytes is whether they arise from the same stem cells, that change physiology of their response as they come to reside in developmentally older tissue, or instead identify two distinct populations of stem cells that fulfill the different roles of first producing an excess of melanocytes, and then filling in the holes and gaps left by the first mechanism. This question was solved by Tu and Johnson using clonal analysis methods described in more detail below (2010).

Specific ablation of larval melanocytes reveals MSCs are repressed by their targets

A thorough dissection of the mechanisms regulating MSCs outlined in Figure 1-1 requires the development of a simpler system than regeneration of the complex tissues of the adult fin, described above. Ideally, this could be achieved by melanocyte specific ablation, employed in stages of the life history with little or no other role for melanocyte development.

The development of methods to use clinical tattoo-removal lasers on one hand (Yang et al., 2004) or melanotoxic drugs to kill late stage melanoblasts or newly born melanocytes on the other hand (Yang and Johnson, 2006), meets the first of these goals. The relative lack of new melanocytes during the larval stage from 60 hours post fertilization (hpf) through 14 days post fertilization (dpf) (see Figure 1-3) meets the second, and sets the stage for a sensitive dissection of the regulation of the MSC.

One of the most salient features of the embryonic melanocyte is that it is the only darkly pigmented cell in the embryo. One property of dyes such as melanin is that they are efficient at absorbing energy from light. Yang and colleagues hypothesized that if they could deliver sufficient visible light to the embryo, they could specifically heat and kill melanocytes without affecting surrounding tissue (Yang et al., 2004). To achieve this, these investigators tried clinical tattoo-removal lasers. These lasers provide intense visible wavelength light in pulses on the order of 5 nanoseconds. Moreover, the light is delivered in 1–3 mm diameter beams, allowing for exposure of much of the embryo in a single pulse. When 2–3 dpf larvae were irradiated, they showed the typical phenotype of melanocyte cell death, including contraction of dendritic processes in melanocytes in the beam path, followed by their extrusion from the larva. Moreover, when exposed embryos were then incubated with the melanin synthesis inhibitor PTU (see above), the region of the embryo in the beam path remained clear of pigmented melanocytes. Subsequent washout of the PTU resulted in the appearance of melanized melanocytes in the beam path. Following the logic used for demonstrating MSCs in the regenerating fin (above), this result indicated that MSCs support and regenerate missing larval melanocytes (Yang et al., 2004). In this case, and unlike the case for the regenerating fin, the regeneration of melanocytes following melanocyte-specific ablation demonstrates that the larval melanocyte is actively

repressing the MSC, and that this repression is relieved when melanocytes are ablated. Whether this repression is direct between the melanocyte and its stem cell, or instead is mediated by other cells or a MSC niche, remains to be determined.

A more easily applied method of melanocyte-specific ablation is provided by the discovery of the small molecule 4-(4-morpholinobutylthio)phenol (MoTP) that effectively kills embryonic and larval melanocytes. MoTP was first identified in the small molecule screens of (Peterson et al., 2000), that showed that embryos could develop in this drug, but lacked melanocytes. Yang and Johnson subsequently showed that MoTP is a prodrug that is converted by tyrosinase to a cytotoxin (Yang and Johnson, 2006). Tyrosinase is an enzyme that converts tyrosine to melanin and is only expressed at high levels in the melanocyte, thus accounting for the melanocyte specificity of MoTP cell ablation. Following MoTP incubation of melanized larvae, melanocytes retract their dendritic processes and are extruded from the fish, similar to that described for melanocyte death in *kit* mutants (Parichy et al., 1999) and following laser ablation. Unlike the laser ablation discussed above, all the melanocytes in the embryo are killed. As seen in Figure 1-3B, these cells leave behind pigmented detritus. When embryos are incubated in MoTP prior to melanization, (from 14 hpf, Figure 1-3D), the melanoblasts are killed without leaving behind a pigmented detritus, that facilitates subsequent quantitative analysis and enables screens for melanocyte regeneration mutants (below). That MoTP ablation is revealing activity of a MSC is demonstrated by the findings that regeneration melanocytes have undergone at least two rounds of cell division as determined by BrdU incorporation, and that the larvae can be induced to regenerate melanocytes again, with a new round of MoTP exposure (Yang and Johnson, 2006). These results indicate that the melanocyte regeneration observed is not due to

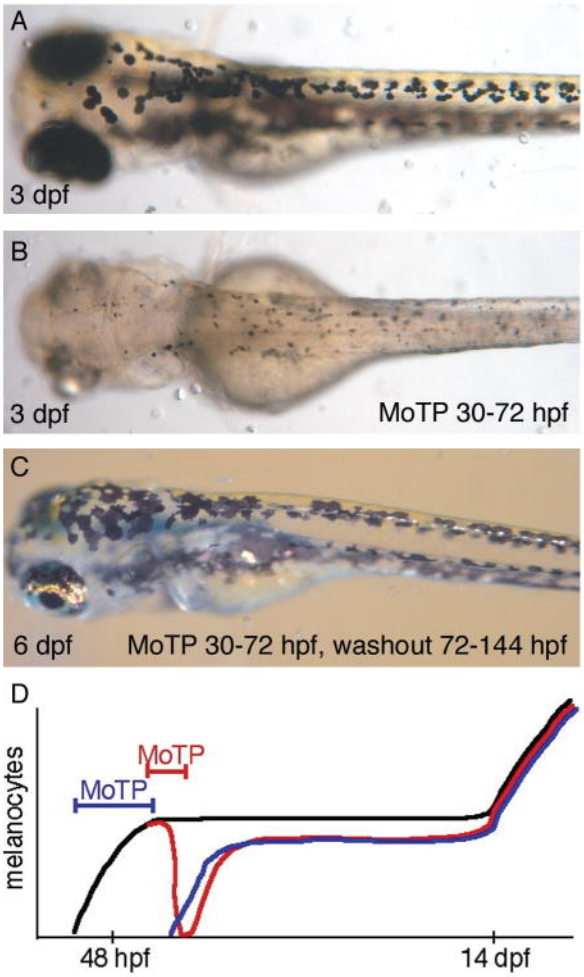

Figure 1-3. MoTP mediated larval melanocyte ablation and regeneration. (A) 3 dpf zebrafish larvae with normal or ontogenetically developed embryonic melanocytes. (B) Similar 3 dpf larvae exposed to melanotoxin MoTP from 30–72 hpf to kill melanocytes. Note faint pigmented detritus. (C) MoTP treated larvae after drug washout and melanocyte regeneration. (D) Schematic shows that wild-type zebrafish (black line) develop embryonic melanocytes prior to 60 hpf, and that between 60 hpf and 14 dpf, few new melanocytes are added to the larval pigment pattern. Treatment with MoTP following melanocyte differentiation (red line) results in rapid melanocyte death. Washout of MoTP results in regeneration of approximately 80% of embryonic melanocyte numbers. Treatment with MoTP before overt melanization (green line) kills developing embryonic melanocytes, but has no affect on melanocyte regeneration. The development of new melanocytes during metamorphosis (beginning at 14 days) is not affected by earlier MoTP treatments.

recruitment of a post-mitotic melanoblast, or poised precursor, and further suggest that the precursors recruited for regeneration are renewed.

Similar drugs, such as 4-hydroxyanisole (4-HA), that are also converted by tyrosinase to cytotoxins, were developed in the 1970s in pursuit of chemotherapies for melanoma (Naish et al., 1988). Unfortunately, in mammals, these drugs were also converted to cytotoxins in the liver, rendering the drugs unsuitable for clinical use against melanoma. In zebrafish, at high concentrations or when applied for more extensive periods, MoTP is also lethal to embryos, perhaps due to less efficient conversion to cytotoxins by other enzymes. Another limitation of MoTP is that it is only effective at killing melanocytes prior to 5–6 dpf, or in newly regenerated melanocytes, that have sufficiently high expression of tyrosinase (Yang and Johnson, 2006). This tends to limit chemical ablation of melanocytes to studies of larval regeneration. Identification of additional drugs that kill old or mature melanocytes in the adult will allow analysis of the regeneration potential of the adult melanocyte, and the properties of the stem cells that support them as well. The development of such drugs is the subject of Chapter 2.

The finding that the larvae recruits from a MSC to repair damage to the embryonic melanocyte pattern raises new questions about the establishment and regulation of the MSCs that generalize to all adult stem cells. One question that comes to mind is whether the MSC is restricted in its lineage, generating only melanocytes. An alternative model is that the MSC activity that we infer from the properties of melanocyte regeneration is actually a multipotent precursor, which can generate all pigment cells, or all neural crest derivatives, such as the neural crest stem cell (Stemple and Anderson, 1992). Solving this question in *vivo* in zebrafish will require the direct identification of the MSC, or lineage and clonal analysis techniques that vitally and persistently mark all derivatives of the neural crest.

An additional problem suggested by these findings is: what is the origin of the MSC in the embryo? There is no reason to doubt that the MSC comes from the neural crest, but there is no particular reason to imagine that it comes from the same lineages as those that give rise to the embryonic melanocytes. An alternative model is that the MSC arises from parallel, or unrelated lineages. This question was addressed by Tryon et al. using clonal analysis methods described below (2011).

Mutant screens for melanocyte regeneration

Although regeneration of the adult caudal fin is easily achieved and several mutant screens have been performed to find mutations that inhibit fin (Johnson and Weston, 1995; Mellgren and Johnson, 2006; Nechiporuk et al., 2003; Poss et al., 2002), no mutants that have specific defects in fin melanocyte regeneration have been found from these screens. Mutants with profound defects in fin melanocyte regeneration, such as *kit*, were identified first as mutations that affect the embryonic pigment pattern (Johnson et al., 1995b). Moreover, it is likely that many of the genes that control the MSC are also required for viability of the embryo, and die before adult stages. A fine scale genetic dissection of melanocyte regeneration awaited the development of a practical regeneration assay in embryonic or larval stages. To accomplish this, Yang and Johnson developed a larval melanocyte regeneration screen (Yang et al., 2007). This screen combines the MoTP melanocyte ablation and regeneration assay with Early Pressure (EP) parthenogenesis (Streisinger et al., 1981) that allows for homozygosis of newly induced mutations. Unlike classic mutant screens in fruit flies or mice, that require that the investigator first generate sibships segregating the mutation, that are then interbred to generate mutant

animals, EP screens allow the investigator to skip the sibship-building generation, thus saving both time and animal facility space.

An important feature of mutant screens is the mutagenesis itself. Although several mutagenesis protocols have been developed, the most popular are those that target the spermatogonia with the chemical mutagen ethylnitrosourea (ENU) (Mullins and Nusslein-Volhard, 1993; Solnica-Krezel et al., 1994). Thus, adult males are treated with the chemical mutagen, ethylnitrosourea (ENU) for several periods over approximately one month. It is also important to allow the mutagenized males another several weeks before breeding to generate the heterozygous females, to allow the mutagenized spermatagonia to replace the sperm. Because each male has at least several hundred proliferating spermatagonial stem cells, typically each heterozygous F_0 female represents an independently mutagenized genome. Specific locus tests for mutagenesis rates range from one to three new mutations per thousand/loci tested, suggesting that saturation mutagenesis, or finding an average of one mutation per gene that could be revealed by mutation in the screen, can be approached by screening the progeny of approximately 1000 F_0 females. As mutagenesis is an important feature of every mutant screen, efficient and efficacious usage of mutagenized males is important. Calculations for the number of spermatagonia in zebrafish males for better screen design appear in Chapter 4.

Another important feature of the larval melanocyte regeneration screen is that following ablation with the drug MoTP, melanocytes regenerate, as discussed above. In Figure 1-3B, we show the detritus of dying melanocytes that were allowed to partially pigment prior to MoTP ablation. In such ablations, the dying melanocytes and detritus are typically extruded from the fish. However, for screening purposes, such detritus may obscure mutants that fail to regenerate melanocytes. Our experience is that adding MoTP prior to overt differentiation of the melanocyte

also kills developing melanocytes. Because these have not yet made melanin, the detritus of their death does not confound identification of mutants that fail to regenerate melanocytes. Such mutants might also be due to simple defects in ontogenetic development, which will be revealed if one-half the haploid embryos that were set aside from the clutch develop with ontogenetic defects. Unlike normal sexual crosses, where Mendelian ratios of 25% are expected for mutants, the ratios in EP half-tetrad clutches can range from 5%, for some telomeric loci, to 50% for loci near centromeres. A more thorough discussion of half-tetrad genetics in zebrafish is provided by Johnson et al. (Johnson et al., 1995a).

Regeneration is not ontogeny

A reasonable expectation of the genetic requirements for regeneration is that many of same genes that promote the development of the cells or tissue will also have similar roles in its regeneration. Differences in genetic requirements between ontogenetic formation of a tissue and its regeneration might then reflect mechanisms that act specifically in one or the other. One example comes from the regeneration-specific defect of the temperature-sensitive fin regeneration mutation, *reg6* (Huang et al., 2003; Johnson and Weston, 1995). This mutant has specific defects in branching morphogenesis used in growing the vascular plexus of the regenerating fin. Since ontogenetic growth of the fin proceeds without a vascular plexus and with little role for branching morphogenesis, the regeneration specificity of the mutation is explained by its role in a regeneration specific mechanism. Similarly, we can expect that identification of melanocyte regeneration mutations may identify mechanisms specific for regulating the stem cells that support the melanocyte pattern, or alternatively, identify differences in how melanocytes differentiate during ontogeny and regeneration.

One such mutation that differentiates between melanocyte ontogeny and regeneration is the temperature-sensitive allele of the *kit* receptor tyrosine kinase (*kit*-ts) (Rawls and Johnson, 2001). This allele was discussed above to help show that *kit* is not involved in establishing the stem cell population that regenerates melanocytes in the regenerating fin, but instead is involved in recruiting the stem cell or differentiating the regeneration melanocytes (Rawls and Johnson, 2001). In the adult fin, the requirement for *kit* in ontogeny and regeneration appear identical. In contrast, when embryonic melanocytes are ablated in the *kit*-ts mutant, either by laser or by MoTP, melanocytes largely fail to regenerate, even when embryos are held at the permissive temperature (Yang and Johnson, 2006; Yang et al., 2004). Note also that melanocytes indeed develop in mutants bearing either null or temperature-sensitive alleles of *kit*. Thus, the requirement on *kit* for melanocyte differentiation is specific to regeneration melanocytes, or to various adult melanocyte populations. The differential role of *kit* in ontogeny and regeneration is explored in Chapter 3.

Two additional melanocyte regeneration-specific mutants were identified in a melanocyte regeneration screen as described above (Yang et al., 2007). Mutants for *eartha* and *julie* develop embryonic melanocytes, but fail to regenerate them after MoTP ablation. In situ expression analysis for dopachrome tautamerase (dct), a gene that promotes melanin formation and marks late melanoblasts, show that the *eartha* mutants accumulate dct-positive melanoblasts but fail to differentiate them into pigmented melanocytes. Closer examination of *eartha* mutants in ontogenetic development revealed that embryonic melanocytes begin to melanize normally, but fail to fully darken. Transplant experiments showed that the *eartha* gene acts cell autonomously in the melanocyte to promote this darkening. Positional cloning of the *eartha* gene showed that it is a defect in the enzyme glutamine:fructose-6-phosphate aminotransferase. This enzyme is the

first step in the hexosamine biosynthesis pathway, that are used either in long chain sugars in the extracellular matrix, or monomeric modifications that affect activity of specific proteins. Not surprisingly, the *eartha* mutation is pleiotropic, with defects in synthesizing the cartilage of the jaw and late larval lethality. The finding that *eartha* acts in the melanocyte tends to rule out roles in the extracellular matrix as that responsible for the regeneration defect and raises the possibility that *eartha*-dependent glycosylation of a specific protein may function to promote early differentiation steps in regeneration, that acts at late stages in ontogenetic development of embryonic melanocytes (Yang et al., 2007).

Similarly, mutants for *julie* have defects specific to melanocyte regeneration that are not shared by embryonic melanocytes. Unlike *eartha* mutants, *julie* mutants fail to accumulate dct-positive melanoblasts, indicating an earlier role, perhaps in recruitment from the MSC. Positional cloning of the *julie* mutation showed that it is a defect in skiv2l2 (Yang et al., 2007), the vertebrate ortholog of yeast MTR4 gene, an ATP-dependent RNA helicase thought to be involved in RNA processing or degradation through the exosome (Bernstein et al., 2008). Like *eartha* mutants, *julie* is pleiotropic, with general defects in cellular proliferation during larval stages. In situ expression analysis of skiv2l2 in larval zebrafish shows it is expressed similarly to the cell proliferation marker pcna, especially in the brain and eyes, regions that largely fail to grow in *julie* larvae after 3.5 dpf. Consistent with defects in general cellular proliferation, *julie* mutant larvae fail to regenerate their tails following amputation (Yang et al., 2007). Thus, here the regeneration-specific requirement for *julie* tempts us to speculate that the difference between ontogeny and regeneration results from whether there is an adult stem cell-like intermediate in the affected lineage. One possibility that explains the apparently normal appearance of *julie* mutants through embryonic development (through 3.5 days) is that most or all of the embryonic

cells develop without an adult stem cell-like intermediate, and that cell division following an adult stem cell requires the function of the skiv2l2 RNA helicase.

MSC development may be revealed by pigment pattern metamorphosis mutants

Developmental biologists have long noted that the adult pigment pattern of poikilotherms such as fish or amphibians differs strikingly from that of embryonic or larval patterns (Niu and Twitty, 1950). This has led to the notion that the embryo sets aside undifferentiated precursors, that are then recruited during metamorphosis, to generate the adult pattern. In zebrafish, this pigment pattern metamorphosis begins at approximately 14 dpf, continuing through 4 weeks, at which time the transition to adult pattern is complete and the fish look like small adults. Because these fish continue to grow and add melanocytes to their pattern throughout their lives, it is likely that a self-renewing stem cell is responsible both for the new melanocytes that arise during metamorphosis and the new melanocytes that arise during growth. This has led Parichy and his colleagues (Budi et al., 2008; Parichy et al., 2000; Parichy et al., 2003; Quigley et al., 2004) to explore how stem cell regulation is responsible for generating new cells in zebrafish metamorphosis, or responsible for the different deployment of new melanocytes observed in closely related species. Of particular interest are the mutants *puma* and *picasso* (Budi et al., 2008; Parichy et al., 2003). Each of these mutants appears identical to wild-type individuals during embryonic and larval stages, but show deficits in recruiting new melanocytes upon reaching the onset of pigment pattern metamorphosis (2 weeks). Interestingly, *puma* was isolated in screens for temperature-sensitive metamorphosis (Parichy et al., 2003). In this mutant, the melanocyte deficit is partially suppressed when fish are allowed to mature more slowly at the

permissive temperature, or when growth was slowed by limiting nutrition, leading to the model that the mutant defect was slow expansion of the MSC population during larval growth.

A second pigment pattern metamorphosis mutant, *picasso*, shows temperature and growth rate independent defects in generation of new melanocytes at metamorphosis. Positional cloning revealed a defect in the EGF receptor-like tyrosine kinase gene *erbb3b* (Budi et al., 2008). Mutants in this gene have also been described for their defects in glial cell development (Lyons et al., 2005). In each study, analysis of the mutant phenotype was aided by the availability of drugs that specifically block the function of erbb receptor tyrosine kinases. Because of the role of EGF receptor and its erbb homologs in a variety of cancers, several highly specific inhibitors of erbb receptor functions have been developed by the drug industry. Interestingly, only when these drugs are applied to zebrafish embryos between 14 and 22 hours (about the time when neural crest cells are migrating into the periphery) is the metamorphosis melanocyte deficit observed (Budi et al., 2008). Thus, the early time of drug action suggests that it blocks the establishment of the MSC population. This was proven by Hultman et al. by showing that while the *erbb3b* mutant has normal ontogenetic melanocyte development, it regenerates very few melanocytes (2009). Thus, this mutant reveals both a differential requirement for ontogeny form regeneration, and that adult pigment pattern mutants may also affect larval stem cells.

Clonal analysis reveals stem cell properties

Clonal lineage analysis involves marking a single cell to follow the progeny of that cell. I will hereafter refer to that simply as clonal analysis. Clonal analysis methods can range from injecting a dye into a single cell (Raible et al., 1992) to quite complicated genetic means (Livet et

al., 2007). Similarly, the questions answered using clonal analysis vary greatly. Here I will focus on questions involving stem cells and mentioned above.

Clonal analysis allowed Tu and Johnson to solve the relationship between the two regenerative melanocytes following adult fin amputation mentioned above (2010) utilizing the Tol2 transposable element (Kawakami et al., 2004). The success of the Tol2 transposable element (Kawakami et al., 2004) in zebrafish has led to great advances in clonal analysis. Clonal analysis can also be simplified through tissue specificity of the method of marking the cells. A common way to achieve this is to put GFP under a tissue specific promoter. To make clones specifically in the melanocytes, a portion of the fugu promoter for *tyrosinase-related protein 1* (f*tyrp1*) that drives expression specifically in the zebrafish specifically in the melanocytes and in the retinal pigmented epithelium (Zou et al., 2006) is used. Tu and Johnson injected f*tyrp1*>GFP plasmid at the 1-2 cell stage to generate clones in fish carrying a temperature-sensitive allele of the *kit* receptor tyrosine kinase (*kit*-ts) (Rawls and Johnson, 2001). These fish were reared at permissive temperatures and screened for clones in the fin. They amputated these fins and allowed regeneration to occur at the permissive temperature. The clones regenerated, establishing ontogeny and primary regeneration melanocytes as being related (Tu and Johnson, 2010). They then performed a second amputation of these fins and allowed regeneration to occur at the restrictive temperature, where the only regenerative melanocytes would be the secondary regeneration melanocytes. They again observed clone regeneration, concluding that ontogeny, primary regeneration, and secondary regeneration melanocytes in the fin (Tu and Johnson, 2010).

To solve the relationship between larval ontogenetic and larval regeneration melanocytes, Tryon et al. (2011) followed a similar methodology to Tu and Johnson (2010). Instead of

screening for clones in the adult fin, Tryon et al. screened for melanocyte clones at 3 dpf. Larvae were then treated with 4-HA to ablate the ontogenetic melanocytes, washed out of 4-HA, and allowed to regenerate melanocytes. The larvae were then rescreened for clones, and a majority of ontogenetic clones also developed regeneration clones (Tryon et al., 2011). They concluded that the ontogenetic melanocytes and the melanocyte stem cell were closely related by lineage (Tryon et al., 2011).

Clonal analysis can also be used to study specific aspects of the regeneration paradigm of Figure 1-1. One example solved the renewal of the intestinal stem cell (Snippert et al., 2010). By modifying the "Brainbow" construct (Livet et al., 2007), every intestinal stem cell and its progeny could be uniquely identified. By examining intestinal crypts after various time frames after clone induction, the conclusion was that stem cell renewal occurred randomly from all daughter cells from all intestinal stem cells within the crypt (Snippert et al., 2010). Clonal analysis techniques, using the tools of Tu and Johnson and Tryon et al., will be used extensively in Chapter 3 to analyze larval melanocyte stem cells.

ACKNOWLEDGEMENTS

We thank Keith Hultman and Rob Tryon for help with figures and for reading the manuscript. This work was supported by NIH grant GM56988 to SLJ.

Chapter 2

Neocuproine ablates melanocytes in adult zebrafish

Adapted from

Thomas O'Reilly-Pol and Stephen L. Johnson (2008)

Zebrafish 5(4): 257-264

ABSTRACT

The simplest regeneration experiments involve the ablation of a single cell type. While methods exist to ablate the melanocytes of the larval zebrafish,(1,2) no convenient method exists to ablate melanocytes in adult zebrafish. Here, we show that the copper chelator neocuproine (NCP) causes fragmentation and disappearance of melanin in adult zebrafish melanocytes. Adult melanocytes expressing eGFP under the control of a melanocyte-specific promoter also lose eGFP fluorescence in the presence of NCP. We conclude that NCP causes melanocyte death. This death is independent of p53 and melanin, but can be suppressed by the addition of exogenous copper. NCP is ineffective at ablating larval melanocytes. This now provides a tool for addressing questions about stem cells and the maintenance of the adult pigment pattern in zebrafish.

INTRODUCTION

Understanding adult stem cells and their regulatory mechanisms is aided by tools that manipulate or ablate the tissue the stem cell monitors. We are interested in the regulation of the melanocyte pattern and precursors or stem cells that may sustain it at various stages of the life cycle in zebrafish. We have previously developed laser protocols (Yang et al., 2004) or drugs (Yang and Johnson, 2006) that allow us to specifically ablate larval zebrafish melanocytes that subsequently regenerate. Amputation of adult caudal fins is followed by fin regeneration with concomitant regeneration of the fin melanocyte stripes. In each case, we have inferred the existence of melanocyte stem cells (MSCs) that support the melanocyte pattern. A mammalian melanocyte stem cell (MSC) has also been identified in the hair follicle (Osawa et al., 2005).

Genetic analysis of melanocyte regeneration following chemical ablation in larvae (Yang et al., 2007) or in the regenerating caudal fin (Rawls and Johnson, 2000) has provided several insights into mechanisms that regulate the MSC, including identifying differences between ontogenetic and regenerative development. However, each of these systems also has limitations for the study of stem cell regulation. For instance, experiments on larval melanocyte regeneration must be completed before the onset of metamorphosis, approximately 14 days post fertilization (dpf), to ensure that the new melanocytes are regenerative and not part of the wave of new melanocytes that develop upon metamorphosis. Thus, regeneration experiments in the larvae are currently limited to two rounds of ablation and regeneration. Moreover, many of the mutations that affect the adult pigment pattern in zebrafish have little or no effect on the embryonic or larval melanocyte. The ability to reliably ablate melanocytes from the adult body stripes would both allow for multiple rounds of melanocyte regeneration and also allow us to

exploit the richness of mutations that affect adult pattern (Budi et al., 2008; Johnson et al., 1995b; Lopes et al., 2008; Parichy et al., 2000; Parichy and Turner, 2003) in studying the mechanisms that regulate the melanocyte stem cell.

The small molecule MoTP that we previously described (Yang and Johnson, 2006) that ablates larval melanocytes is a prodrug that is converted by the melanin synthesizing enzyme tyrosinase into a cytotoxic phenolic compound. The high specificity of ablation of melanocytes is explained by the fact that only developing or newly pigmented melanocytes express sufficiently high levels of this enzyme to produce cytotoxic levels of the phenolic product. One limitation of MoTP for melanocyte ablation is that it fails to ablate mature melanocytes that no longer express high levels of tyrosinase (Yang and Johnson, 2006). Thus, embryonic melanocytes become largely refractile to ablation by MoTP after approximately 6 days post-fertilization, and most adult melanocytes are also resistant to MoTP mediated ablation. The laser protocol described for ablation of embryonic melanocytes (Yang et al., 2004), that utilize the intense flux of dermatology tattoo removal lasers, is effective in ablating melanocytes from the adult pigment stripes, but is less specific than in the embryo. Laser treatment of the adult body stripe also results in the ablation of the yellow xanthophores as well as causing some collateral tissue damage (O'Reilly-Pol, unpublished data). Identification of a small molecule or drug that specifically ablates mature melanocytes, particularly in the adult body stripes, and has no effect on xanthophores is now required to fill this gap in our ability to ablate melanocytes and study the potential of MSCs to regenerate the adult melanocyte population.

In this chapter, we describe the identification of a drug, neocuproine (NCP), that specifically ablates the melanocytes of adult zebrafish. We have previously shown that NCP, a copper chelator, prevents tyrosinase function and melanin synthesis in the zebrafish embryo

(Mendelsohn et al., 2006). In adult zebrafish, we show that the melanocytes exhibit the same sequellae of death (contraction and fragmentation) as observed in larval melanocyte ablation, as well as in other adult teleosts (Parichy et al., 1999; Sugimoto et al., 2000; Yang et al., 2004). This effect of NCP is suppressed by exogenous copper, suggesting that it acts through copper depletion to ablate melanocytes. We also show through the use of *albino* fish that melanin is not necessary for this ablation. Neocuproine now provides us with a tool to specifically ablate melanocytes in the adult to allow us to explore the regulation of the MSC in the adult zebrafish.

METHODS

Fish stocks and husbandry

Standard fish husbandry protocols were followed (Westerfield, 1995). Wild type fish stocks were largely AB. *j999a* is a transgenic line containing a 7.7kb promoter fragment from upstream of the fugu *kit* gene cloned into the tol2 transposon vector and driving eGFP, inserted into the genome as previously described (Kawakami et al., 2004). *Melanophilina*^{j120} (Sheets et al., 2007) mutants were used in the generation of transgenic and mosaic fish (see below) as the melanosomes are concentrated in the center of the cell, thus allowing visualization of eGFP in most of the cytoplasm. *Albino*^{b4} and *p53*^{zdf1} were obtained from the Zebrafish International Resource Center (NIH P40 grant RR012546).

Drug treatments

4-(4-morpholinobutylthio) phenol (MoTP) was custom synthesized by Gateway Chemical Technology (St Louis, MO). *N*-phenylthiourea (PTU) (catalog number P7629), epinephrine (cat. E4250), neocuproine (NCP) (cat. N1501), bathocuproinedisulfonate (BCS) (cat. B1125), and antabuse (cat. T1132) were obtained form Sigma-Aldrich (St. Louis, MO). All drugs were changed every 2-3days. Neocuproine was used at 750nM, except when noted as otherwise. Epinephrine was used at 1mg/mL. NCP and antabuse stock solutions were made in DMSO, and diluted to a final concentration in less than 0.1% DMSO.

As an internal control to demonstrate the effectiveness of copper chelation by NCP, PTU, BCS, and antabuse, a simultaneous partial amputation of the caudal fin was performed. In each

case, the concentration of drug used was sufficient to block most or all melanin synthesis in the regenerating fin. Treatment with vehicle (0.1% DMSO) allowed full melanin synthesis.

Tyrp1:*eGFP*

The tol2 transposon construct used to generate *tyrosinase-related protein 1* (*tyrp1)*:eGFP mosaic and transgenic fish was previously described (Zou et al., 2006). The methods for generating mosaic fish and stable transgenics have also been described (Kawakami et al., 2004). Quantification of melanocyte loss was performed by counting along the middle stripe of the caudal fin for a length of 3 fin ray segments in the proximal portion of the fin.

Photography

All pictures were taken with a ProgRes C14 camera with accompanying software (Jenoptik Laser. Optik. Systeme., Jena, Germany) on a Nikon SMZ 1500 Stereomicroscope (Tokyo, Japan). An X-cite 120 Fluorescent Illumination System (Exfo Life Sciences, Ontario, Canada) was used for fluorescent excitation of eGFP. In some cases (Fig. 1A-F), fish were euthanized and mounted in 1% agar on 10cm Petri dishes. They were then photographed through the bottom of the plate to reduce glare. All other pictures were of live, unmounted fish taken with incidental light. Pictures were edited with Photoshop CS2 (Adobe Systems Incorporated, San Jose, CA).

RESULTS

Knowing that neocuproine (NCP), a copper chelator, affects copper-dependent processes including melanin synthesis in the zebrafish embryo (Mendelsohn et al., 2006), we wanted to see the effects of disrupting copper homeostasis in adult zebrafish. Adult zebrafish were treated with 750nM NCP, a concentration below the threshold necessary for blocking melanin synthesis in the embryo. We found that by 10 days of treatment, fish were largely devoid of melanin in their body stripes and fins (Fig. 2-1B). When fish were returned to fresh water, the pigment pattern was reconstituted within 4 weeks after drug washout (not shown).

We wanted to better understand the depigmentation process, so we observed the morphology of melanocytes undergoing treatment with NCP. Melanocytes start out with their melanin (melanosomes) fully dispersed and have many pigmented dendritic processes (Fig. 2-1C). By three days of treatment in 750nM NCP, all melanocytes have lost pigmented processes and the melanin is more contracted overall (Fig. 2-1D). Some of the melanocytes have discreet puncta of melanin. After five days of treatment, the melanin appears hazy, as if it is no longer cellular (Fig. 2-1E). At 7 days, most of the melanin is gone, leaving only scattered dark puncta (Fig. 2-1F). After 10 days, nearly all the melanin has been cleared, although there are areas that appear resistant to neocuproine such as some scale melanocytes and the distal tips of the fins. We suggest that this sequence of events reflects the death of melanocytes followed by mechanisms to clear the detritus (see Discussion).

The observed phenotypes at 3 days intrigued us. Melanosomes contract when exposed to epinephrine, with the melanosomes moving along microtubule networks towards the center of

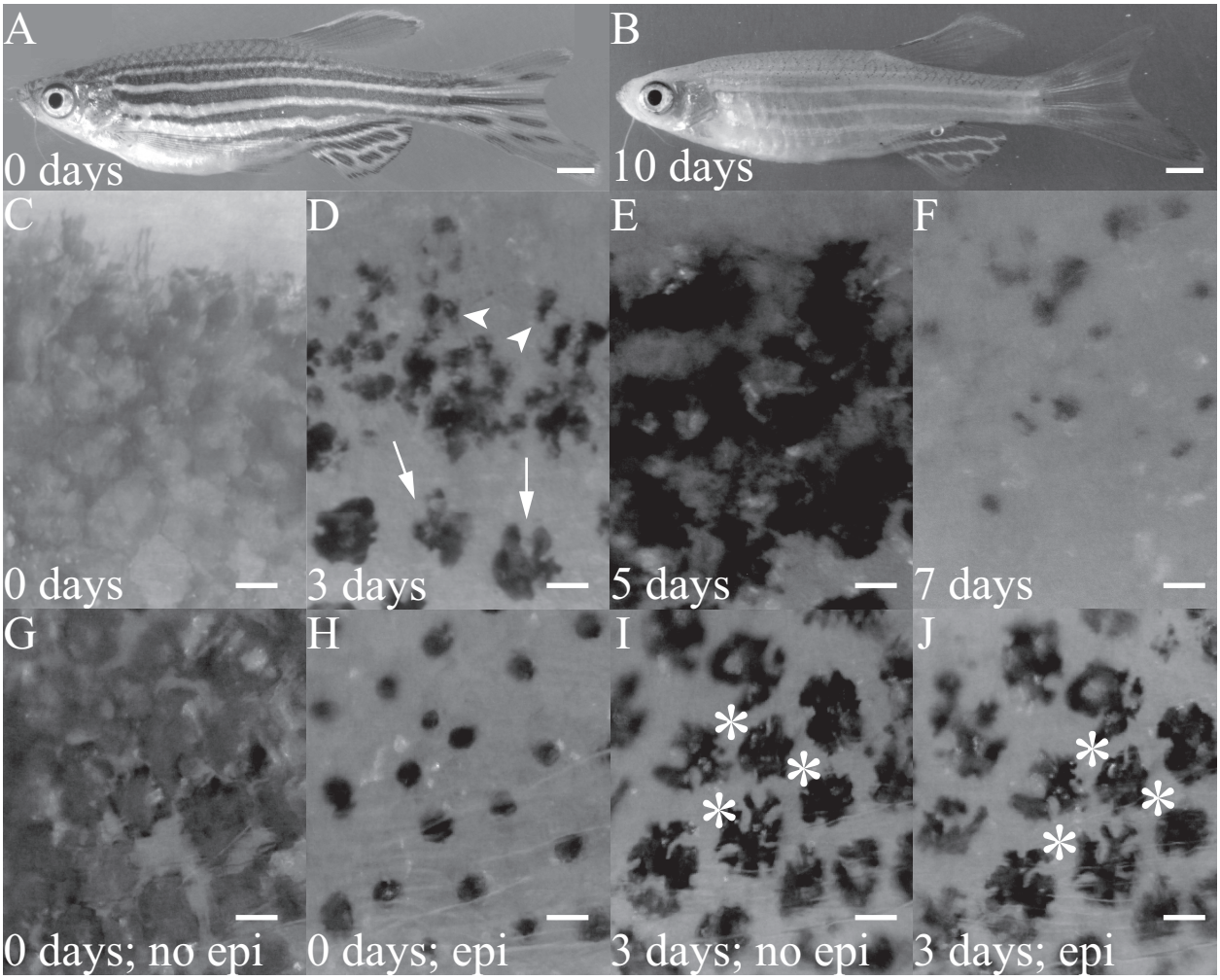

Figure 2-1. Progression of melanocyte morphology during exposure to NCP. (**A**) An untreated, fully pigmented fish. (**B**) A fish after 10 days of NCP treatment. It is almost entirely devoid of melanin in the body stripes and fins. (**C–J**) Close-ups of melanocyte stripes after treatment with NCP. Melanosomes are fully relaxed, and there are many pigmented processes before treatment with NCP (**C**). After 3 days, the melanin has contracted to result in lobular melanin masses (**D**, arrows). Some melanocytes have begun to fragment (**D**, arrowheads). After 5 days of NCP, melanin appears as if acellular (**E**). After 7 days, most of the melanin has been cleared, leaving scattered granules (**F**). Fish untreated with NCP prior (**G**) and after exposure (**H**) to epinephrine. Note the contracted melanosomes in (**H**) compared to (**G**) and that these contracted melanosomes are regular and round in appearance. Lobular melanin masses after 3 days in NCP look similar before (**I**) and after exposure (**J**) to epinephrine. Asterisks in (**I**) and (**J**) mark the same melanocytes. Note that there is no change in these melanocytes after epinephrine treatment. Scale bars in (**A, B**) are 1 mm and in (**C–J**) are 100 μm.

the cell (Sheets et al., 2007) (compare Fig 2-1G to 2-1H). Melanin is partially contracted after 3 days of NCP treatment (compare Fig. 2-1G to 2-1I). However, the shapes are different. Epinephrine treatment results in round aggregations of melanin, whereas NCP treatment results in irregularly shaped or lobular melanin aggregates (compare Fig. 2-1H to 2-1J). Moreover, after 3 days of NCP treatment melanin did not noticeably contract in response to epinephrine (compare asterisked melanocytes in Fig. 2-1I to 2-1J). This suggests that the lobular melanin is not an intermediate stage of melanosome contraction.

Loss of* tyrp1:eGFP *expression from melanocytes in NCP treated fish

Next, we used the previously described construct of fugu *tyrp1* promoter driving eGFP (Zou et al., 2006) to make eight mosaic adults with eGFP expression in clones of melanocytes. *Tyrp1* (*tyrosinase-related protein 1*) is expressed exclusively in melanocytes in both fish (Zou et al., 2006) and mammals(Jackson et al., 1990). Following 1 day in 750nM NCP we found that eGFP expression was no longer detectable in a majority of melanocytes (182/194 cells). Some of these cells retain a small amount of eGFP. However, the eGFP no longer surrounds the melanin mass as it did prior to NCP treatment (Fig. 2-2B arrowhead). A few cells (12/194, arrow Fig. 2-2B) retain all of the eGFP expression, suggesting they are resistant to NCP. We note that these melanocytes appear smaller than the melanocytes that lost eGFP expression following NCP treatment. Thus, the resistant melanocyte may be younger developmentally and may need to mature to become NCP-sensitive (discussed below).

We also note that two of the mosaic adults contained xanthophore clones adjacent to melanocyte clones. Xanthophores are a related, but different, type of dermal pigment cell that does not contain melanin. Although stable transgenic lines for the *tyrp1*:eGFP construct do not

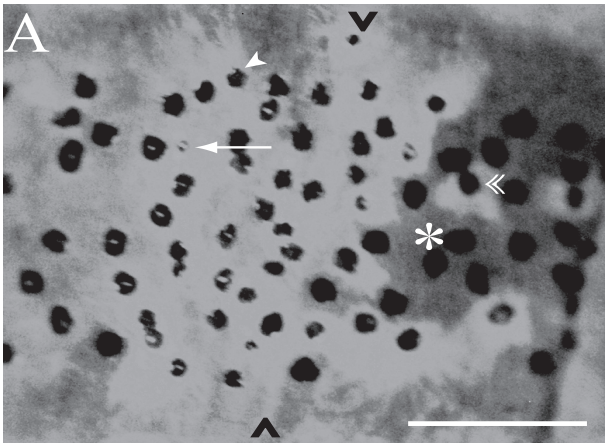

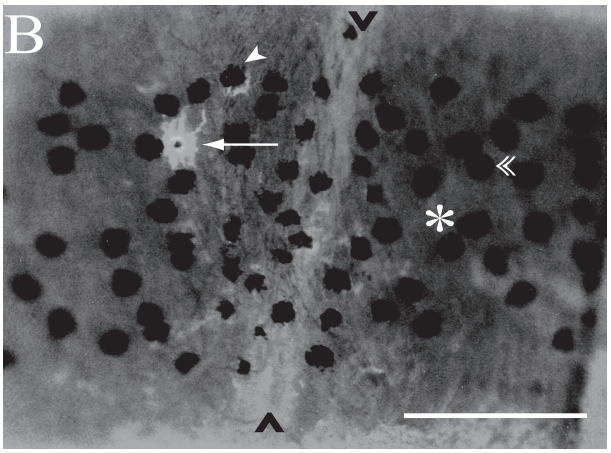

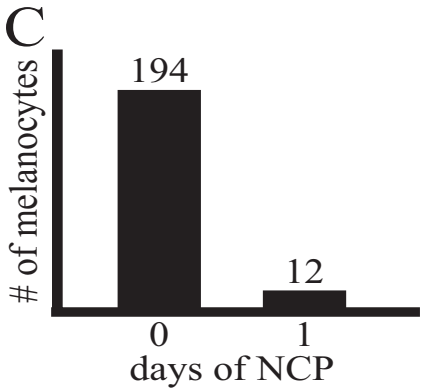

Figure 2-2. Loss of *tyrp1*:eGFP from mosaic adults after treatment with 750 nM NCP. (**A**) 0 day. (**B**) 1 day. The arrow indicates one melanocyte that fully retained eGFP after treatment. The arrowhead indicates one melanocyte that partially retained eGFP after treatment. The eGFP no longer surrounds the melanin, and is not in dendritic processes (compare with the arrow). The double arrowhead indicates a melanocyte that lost all eGFP expression (compare with arrow and arrowhead). The asterisk indicates melanocytes that were initially negative for eGFP. The black carats mark the boundary of the myotome, which has mild autofluorescence. (**C**) Quantification of eGFP^{+} melanocytes in eight mosaic fish before and after NCP treatment.

express eGFP in their xanthophores, we occasionally observe mosaic expression in xanthophores of injected animals. These mosaic animals provide an opportunity to ask whether NCP affects transgene expression in another cell type. In these fish, the eGFP expressing xanthophores maintained eGFP expression after neighboring eGFP-expressing melanocytes had extinguished their expression and fragmented (not shown).

To further explore the loss of eGFP we treated transgenic adult expressing *tyrp1:eGFP* with NCP. In the proximal caudal fin, approximately 98% (1174/1195, n=4) of the melanocytes lost eGFP expression after one day of NCP treatment. The minority of melanocytes that continued expressing eGFP at 24hrs persisted their eGFP expression through 4 days of drug treatment (not shown).

***Melanocyte specific loss of* eGFP**

To determine the specificity of NCP for melanocytes, we utilized the transgenic line *j999a*. This line contains eGFP under the control of the fugu *kit* promoter. Expression, however, is mosaic, resulting in eGFP expression in many cells not known to express *kit*, including skin and muscle. As above, treating these fish with NCP for one day ablates eGFP expression in melanocytes. In contrast, eGFP expression persists unperturbed in all skin and muscle clones of NCP treated fish (not shown).

Brief exposure to neocuproine

As *tyrp1*:eGFP expression was extinguished after one day, we next wanted to see if the melanocytes were capable of recovering from this brief exposure to NCP. We treated fish with NCP for one day, and then washed them into fresh water. To our surprise, not only did

melanocytes progress as if they were still in drug, but the events were accelerated. After 2 days of washout, they more closely resembled fish that had been in NCP continuously for 7 days (compare Fig. 2-3C to 2-1D and 2-1F). It is unclear why removal of NCP speeds progression of the melanocyte ablation, but this may reveal a role for copper in the clearing of melanocyte detritus. Nevertheless, this result reveals that adult melanocytes have committed to death within 24 hours of NCP exposure.

***Independence of NCP-induced death from* p53**

We wanted to know if the observed melanocyte death went through classic apoptotic pathways or a different mode of cell death (i.e. non-classical apoptosis or necrosis). As many of the ways to assess apoptosis (TUNEL staining, acridine orange staining, etc.) are difficult to perform in the melanocyte, as the melanin prevents label detection, we instead used fish with a homozygous mutation in *p53* (Berghmans et al., 2005). This mutant is defective for apoptosis (Berghmans et al., 2005). Wild type (WT) and *p53* mutant fish were treated for 1 day with NCP. After 2 days following NCP washout, WT (Fig. 2-3A, C) and *p53* mutants (Fig. 2-3B, D) are indistinguishable: both genotypes retain only scattered puncta of melanin (Fig. 2-3C, D). This indicates that melanocyte ablation following NCP treatment is not via *p53*-mediated apoptosis.

Melanin is not required for NCP-induced melanocyte ablation

We wondered whether melanin was a necessary component of the neocuproine mediated ablation, as xanthophores, a pigment cell lacking melanin, were unaffected by neocuproine. We used the *albino* mutant, which has unpigmented melanocytes. To test this notion, we crossed the *tyrp1:eGFP* transgene into *albino* stocks to allow us to observe melanocytes (Fig. 2-4A). When

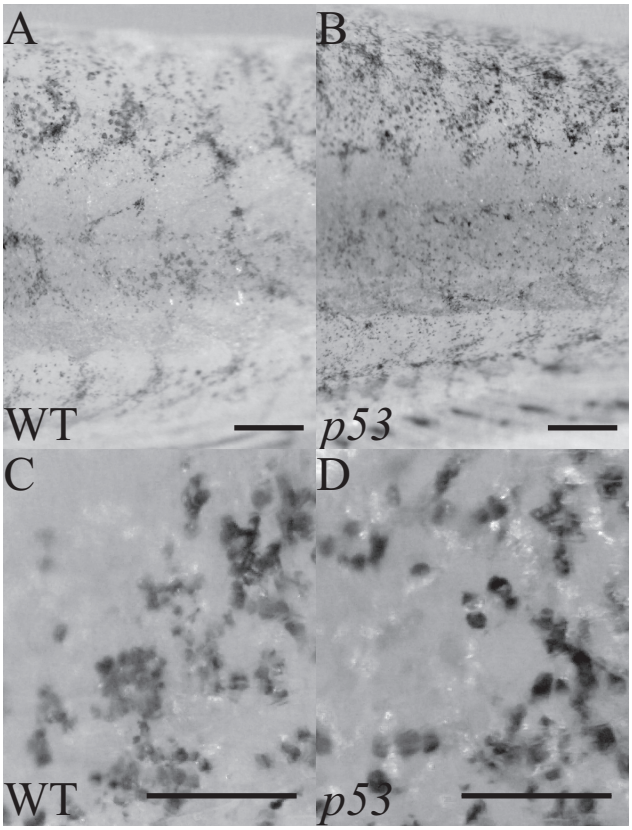

Figure 2-3. Melanocyte loss in *p53* mutants. Fish were treated for 1 day in 750 nM NCP and washed into fresh water for 2 days. WT (**A, C**) and *p53* mutants (**B, D**) are equally affected by the NCP treatment. The melanocytes have already fragmented and begun to be cleared (**C, D**). Scale bars in (**A, B**) are 500 μm and in (**C, D**) are 100 μm.

we treated these fish with NCP we found that eGFP expression was largely gone by 24 hours (Fig. 2-4B), and completely absent from *albino* fish by 5 days of NCP treatment (Fig. 2-4C). This shows NCP does not require melanin or functional melanin synthesis to cause melanocyte ablation.

Role of copper during neocuproine-induced melanocyte ablation

We next wanted to know what the effective concentration of neocuproine was for melanocyte ablation. We discovered that concentrations greater than 1μM NCP were highly toxic to fish at seven days (Table 2-1), placing these doses outside of the effective range. 750nM NCP caused approximately 20% fish lethality, with negligible death at all lower concentrations of NCP (Table 2-1).

To assess the effects of NCP on induced melanocyte ablation, we examined fish 7 days after treatment, putting fish into one of three categories based on the pigmentation: unaffected; half-affected; or completely affected. Half-affected fish lose approximately one quarter to half of their melanocytes from the middle stripe. Typically, depletion was strongest in the caudal half and proceeded rostral in completely affected fish. At concentrations over 500nM, all fish are completely affected by 7 days of neocuproine treatment. Similarly, at 300nM, most fish are also completely affected. However, at 100nM the treated fish are distributed among the three categories. At 30nM, a large majority of the fish is unaffected, with no effect seen at 10nM (Table 2-1). Thus, we conclude that 500-1,000nM NCP produces the most effective dose for melanocyte ablation, although there is some fish lethality observed at the higher end of this range.

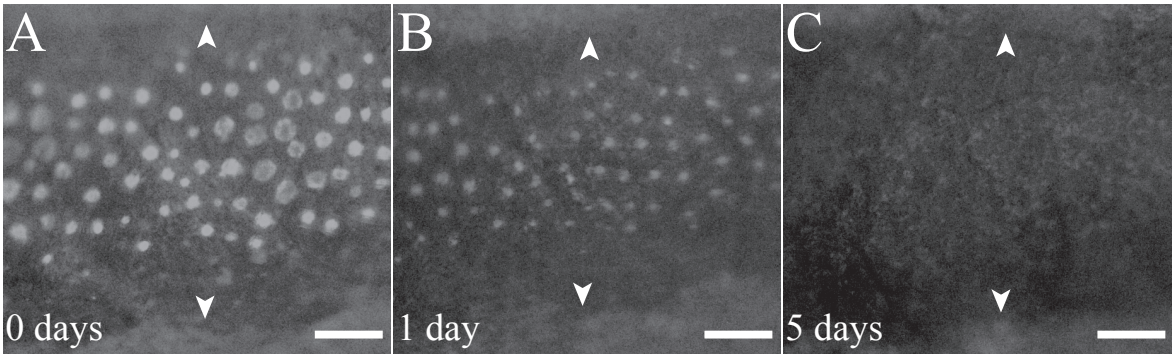

Figure 2-4. Loss of *tyrp1*:eGFP from *albino* transgenics after treatment with 750 nM NCP. (**A**) 0 day. (**B**) 1 day. Note that most of the eGFP signal is lost [compare with (**A**), but some faint eGFP is evident]. (**C**) 5 days. All the eGFP signal is lost. Arrowheads mark the melanocyte/xanthophore stripe boundary. Scale bars are 200 μm.

To test the role of copper during NCP-induced melanocyte ablation, we added 1μM of $CuCl_2$ to fish treated with intermediate concentrations (100 or 300nM) of NCP. At these concentrations of NCP, copper is in excess (approximately 20 or 7 fold excess Cu^{2+}). In each case, the excess copper suppressed the NCP-induced melanocyte death (Table 2-1), thus tending to suggest that NCP acts to ablate melanocytes by depleting the available copper. We note, however, that exogenous copper did increase fish lethality at higher concentrations of neocuproine (Table 2-1), suggesting that in other cells in the fish NCP may exert its lethal effects by inappropriately mobilizing copper.

Effects of other copper chelators

We asked whether other copper chelators could induce melanocyte ablation. We tested bathocuproine sulfate (BCS), an analog of neocuproine, which unlike NCP is cell impermeable, and PTU, a widely used drug that inhibits melanization of melanocytes and shares little structural similarity to NCP. Exposure of fish to these drugs (750nM BCS and 100μM PTU) caused no evidence of depigmentation or melanocyte ablation after 7 days in the drug.

In contrast, the copper chelator antabuse caused weak depigmentation (Fig. 2-5). Antabuse, like PTU, is structurally dissimilar to NCP. Antabuse has been shown to prevent melanin synthesis in larval zebrafish (Mendelsohn et al., 2006). After antabuse treatment (1μM), we found occasional fish (6/14) with gaps (Fig. 2-5B) in the stripe. These gaps are smaller than the half-affected fish described in our dosage testing of NCP (above), and some contained lobular melanocytes (Fig. 2-5C) or melanocyte detritus (Fig. 2-5D). Gaps and the presence of melanocyte detritus are typically never observed in untreated fish.

Table 2-1. Concentration response to neocuproine (NCP) and suppression of NCP by exogenous copper.

Treatment	Affected[a]	Half-affected[b]	Unaffected	Dead
10μM NCP	0	0	0	10
3μM NCP	2	0	0	8
1μM NCP	47	0	0	34
750nM NCP	78	0	0	22
500nM NCP	62	0	0	1
300nM NCP	84	23	1	6
100nM NCP	41	38	34	2
30nM NCP	0	4	61	0
10nM NCP	0	0	20	0
750nM NCP + 500nM $CuCl_2$	0	0	0	30
300nM NCP + 1μ M $CuCl_2$	1	6	105	1
100nm NCP + 1μ M $CuCl_2$	0	0	104	1

[a] Affected fish are missing most or all of their melanocytes of their body stripe. [b] Half-affected fish are missing ~25-50% of the melanocytes in their body stripes.

Effective periods of drug exposure for melanocyte ablation

Now possessing drugs that have been shown to ablate melanocytes in larval (MoTP) and adult (neocuproine) stages we wanted to further define when each of these drugs was melanotoxic (summarized in Fig. 2-6). We treated our transgenic line expressing *tyrp1:eGFP* with NCP or MoTP and scored them for melanocyte morphology (fragmentation, as above) and loss of eGFP fluorescence as metrics for melanotoxicity.

To confirm that neocuproine only prevented pigmentation in embryonic melanocytes, we treated embryos form the *tyrp1:*eGFP transgenic line for two days with MoTP, PTU, and neocuproine before the cells were melanized. All three treatments resulted in unpigmented embryos, but PTU and NCP contained eGFP-positive, melanin-negative melanocytes, showing that for these copper chelators the melanocytes were not ablated. In contrast, MoTP had no eGFP signal, consistent with the previous finding that MoTP kills melanoblasts as well as differentiated larval melanocytes (Yang and Johnson, 2006) (not shown).

We find that MoTP no longer affects melanocytes after 6-7 days post fertilization (dpf). This is consistent with our previous finding that MoTP requires conversion by tyrosinase into a cytotoxin, and that tyrosinase expression decreases after 5dpf (Yang and Johnson, 2006). We find that MoTP ablates melanocytes once again at 15dpf (not shown), which is approximately the onset of metamorphosis when adult melanocytes begin to differentiate and thus should require high tyrosinase activity for pigmentation. In adult fish (>6 months), MoTP shows no discernible effect on melanocytes, even at concentrations higher than the larval threshold or when applied for 7 days.

To explore the effect of NCP on melanocyte survival in larval zebrafish we used NCP at 5μM. This is the minimum dose required to block melanin synthesis in the embryo

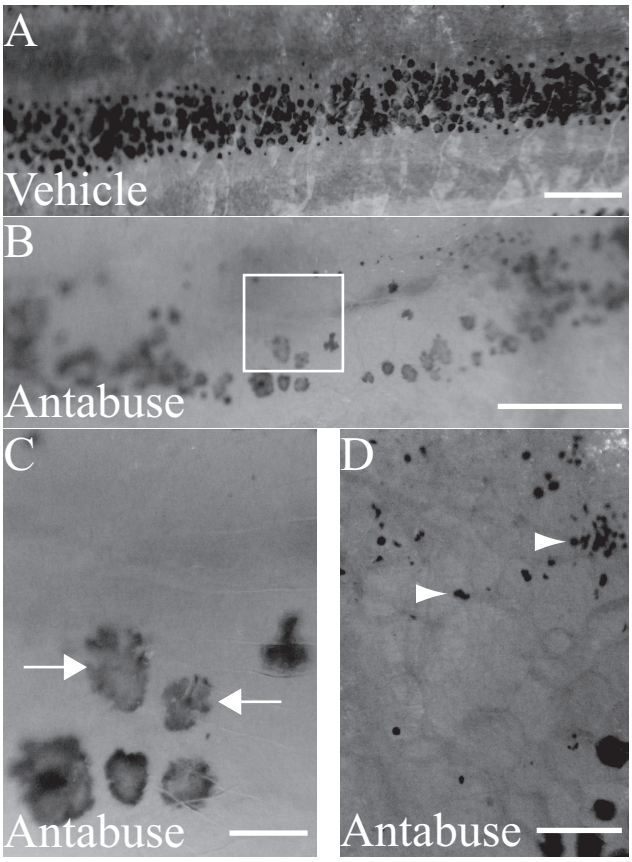

Figure 2-5. Partial loss of melanocytes after antabuse treatment. (A) Vehicle treatment. (B) 10 μM antabuse. Note the large gap in the stripe that is typically not observed in untreated fish. (C) A close-up of the box in (B) showing lobular melanocytes (arrows) (D). A close-up of a similar gap to (B), except with melanocyte detritus (arrowheads). Scale bars in (A, B) are 500 μm and in (C, D) are 100 μm.

(Mendelsohn et al., 2006), and is 10-fold greater than what is necessary in the adult to ablate melanocytes. However, even at this high concentration, we did not observe any morphological changes or loss of eGFP expression in the melanocytes exposed to NCP for any 2-day period between 3 and 15dpf. Similarly, we observed no depigmentation when larval fish were treated with 750nM NCP for 7 days. We first observed NCP-induced melanocyte ablation in fish once they had reached 5 weeks of age. This suggests there is some physiological change in the adult that occurs as it matures that makes it susceptible to ablation by neocuproine.

Neocuproine only ablates melanocytes in mature tissue

The observation that NCP only ablated melanocytes in older fish led us to ask whether this result reflected a global change in fish physiology resulting in NCP sensitivity. Alternatively, the change in sensitivity could reflect the age of the melanocyte or its immediately surrounding tissue. We reasoned that the regeneration of melanocytes in regenerating fins would allow us to test between these models. Accordingly, we amputated fins in the *tyrp1*:eGFP line and allowed them to regenerate for 7 days prior to treatment with NCP. This allowed significant development of new melanocytes in the fin regenerate (Fig. 2-7A and B). The regenerative and ontogenetic melanocytes both expressed eGFP (Fig. 2-7C). After 1 day of NCP treatment, eGFP expression is lost in the older, ontogenetic melanocytes, but not in the younger, regenerative melanocytes (Fig. 2-7D). This result rules out the model that global changes in the adult physiology confer NCP sensitivity. Instead, this result tends to suggest that the melanocytes or the tissue surrounding it must mature to become sensitive to NCP.

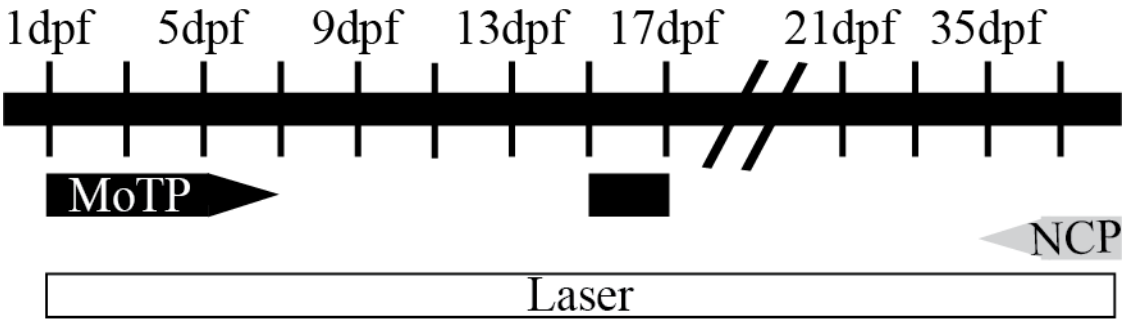

Figure 2-6. Timeline for effective melanocyte ablation. Fish were treated for 2-day periods with either 5 µM NCP or 10 µg/mL MoTP at 1, 3, 5, 7, 9, 11, 13, and 15 dpf and assessed for melanocyte ablation. Fish were treated for 7-day periods with 20 µg/mL MoTP at >180 dpf or 750 nM NCP at 21, 28, 35 dpf, and >180 dpf. The effectiveness of the laser protocol represents a variety of experiments on larval (Yang et al., 2004) and adult (O'Reilly-Pol, unpublished data) fish. Effective periods for each method are designated by the bar under the timeline (black for MoTP, shaded for NCP, and open for laser).

DISCUSSION

We first considered the model that NCP was revealing normal turnover of melanin or melanocytes in the adult. This seems unlikely since we never see these lobular or fragmented melanin clusters that we observe in NCP-treated fish (Fig. 1D) in untreated fish. Additionally, another drug that blocks melanin synthesis, PTU, has been often used in adult zebrafish without any suggestion of revealing melanocyte turnover (Rawls and Johnson, 2000; Rawls and Johnson, 2001). Also, we have kept fish in PTU for up to 5 weeks without affecting pigmented melanocytes (O'Reilly-Pol, unpublished data). Thus, we tend to reject the model that NCP, by blocking melanin synthesis, reveals normal turnover of melanin or melanocyte death in adults. This led us to explore models of NCP inducing melanin turnover (Turnover Model) or melanocyte death (Death Model).

These two models of induced turnover of melanin and melanocytes make testable predictions about the depigmentation of fish. Under the Turnover Model, other cellular components should persist in the presence of NCP. We would expect that a melanocyte expressing eGFP under the control of a melanocyte specific promoter, such as the *tyrp1* or *kit* promoters used, would continue to express eGFP. They do not (Fig. 2), as the Death Model predicts. The continued eGFP expression in multiple cell types during NCP treatment shows specificity for NCP to quench eGFP in the melanocyte. The use of two different promoters tends to rule out loss of eGFP expression from an interaction between NCP and the *tyrp1* promoter. In the amputation experiment, eGFP expression is preserved in the regenerative melanocytes, further establishing that NCP does not generally interact with eGFP or the *tyrp1* promoter. The Turnover Model predicts melanocytes should gradually lose their pigmentation (fade) in the

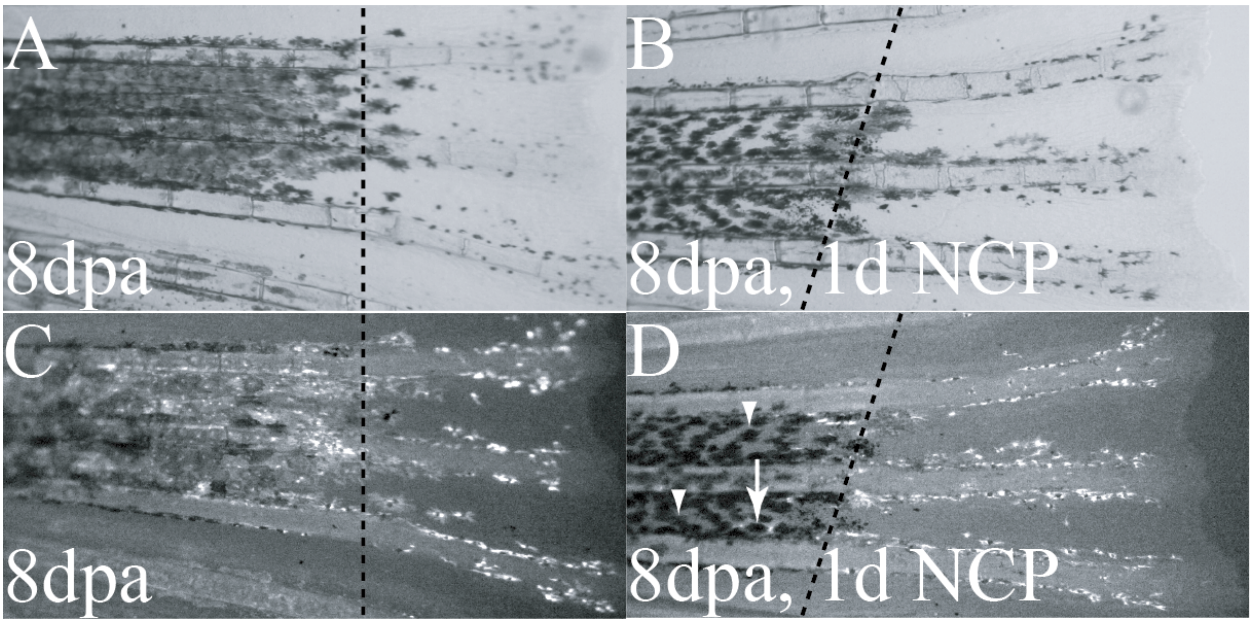

Figure 2-7. NCP does not ablate newly regenerated melanocytes. (**A**) Fish fin carrying transgenic *tyrp1*:eGFP 8 days postamputation (dpa) under white light. The dashed line represents the amputation plane. (**B**) A fish fin carrying transgenic *tyrp1*:eGFP 8 dpa and 1 day of NCP treatment under white light. The dashed line is the amputation plane. (**C**) The same fin as in (**A**), under fluorescent light. Note GFP is on both sides of the amputation plane in all melanocytes. (**D**) The same fin as (**B**), under fluorescent light. Most of the melanocytes proximal (to the left) of the amputation plane have lost GFP expression (arrowheads), although some retain GFP expression (arrow). All of the melanocytes distal (to the right) of the amputation plane express GFP.

presence of NCP while maintaining their overall size, shape, and identity. In contrast, the Death Model predicts that as melanocytes die, they will fragment as previously described (Parichy et al., 1999; Sugimoto et al., 2000; Yang et al., 2004), which they do (Fig. 1C-F). Weaker support comes from the loss of melanocyte sensitivity to epinephrine (Fig. 1G-1I) and commitment to depigmentation after brief exposure to NCP (Fig. 3). Thus, we favor the Death Model. It does remain formally possible that NCP is not inducing melanocyte death but instead exerts multiple effects by beginning a cascade with continuing effects that results in: depigmentation; loss of epinephrine sensitivity; and quenching of eGFP only in melanocytes.

Once we established to our satisfaction that NCP caused melanocyte death, we wondered if this death was classic apoptosis. We could not do this in many of the standard ways. We have been unable to accurately determine melanocyte nuclei in whole mount fish fins or dissected skin. Thus, we were prevented from gauging the presence of pycnotic or TUNEL stained nuclei to assess apoptosis. However, we found identical NCP-induced melanocyte ablation in mutants homozygous for a *p53* mutation, suggesting that whatever type of cell death was occurring , it was not *p53*-mediated apoptosis.

We also explored the role of copper in NCP-induced melanocyte ablation. In the first model, NCP depletes copper from the cell, revealing essential melanocyte-specific copper-dependent protein activity. In a second model, NCP may inappropriately mobilize copper in the cell causing damage from the redox activity of copper. A third model is an off-target, possibly copper-independent, effect of NCP. These models can be partially distinguished by adding exogenous copper. If the first model is correct, the addition of excess copper should suppress the effect. This test was used in larval zebrafish to show that NCP affected melanin synthesis through copper chelation(Mendelsohn et al., 2006). Alternatively, for the second model, adding

exogenous copper should worsen the phenotype. This is the conclusion favored in studies of NCP in HepG2 cells(Tsang et al., 1996) and cultured rat cortical astrocytes(Chen et al., 2008) where copper increases the toxicity of NCP. The third model would probably be unaffected by copper. However binding of copper may change the structure of NCP, and thus also the off-target properties of NCP, so the exact effect cannot be predicted.

Our results that copper suppresses the melanotoxic effects of NCP (Table 1) tend to argue against the second model that purports inappropriate copper mobilization. As we find that a structurally dissimilar copper chelator, antabuse, is also melanotoxic in adults, we tend to argue against our third model for off-target effects. Thus, we favor the first model (copper depletion) for NCP's` mode of action, and that copper is required for the survival of adult melanocytes.

Conclusion

We show that NCP, a copper chelator, ablates adult, but not larval, melanocytes. This melanotoxicity reveals a specific role for copper in the continuing survival of melanocytes. Death of these melanocytes occurs in a manner that is independent of *p53*-mediated apoptosis, and does not require the presence of melanin. Only mature adult melanocytes are affected. This drug now provides a tool for ablating adult melanocytes and exploration of the role of melanocyte stem cells in the maintenance of the adult pattern.

ACKNOWLEDGEMENTS

We thank Erik Madsen for his intellectual contributions, Ahu Turkoz for technical assistance and Chao-Tsung Yang for generating the *j999a* (fugu *kit*:eGFP) transgenic line. We also thank Jian Zou and Xiangyun Wei for the *tyrp1*:eGFP construct. This work was funded by National Institutes of Health grant GM56988 to SLJ.

Chapter 3

Kit signaling is involved in the fate decision for the melanocyte stem cell in zebrafish embryos.

Adapted from

Thomas O'Reilly-Pol and Stephen L. Johnson (2012)

Development (under review)

ABSTRACT

Adult stem cells are crucial for growth, homeostasis, and repair of adult animals. The melanocyte stem cell (MSC) and melanocyte regeneration is an attractive model for studying regulation of adult stem cells. The process of melanocyte regeneration can be divided into establishment of the MSC, recruitment of the MSC to produce committed daughter cells, and the proliferation, differentiation, and survival of these daughter cells. Reduction of *kit* signaling results in dose-dependent reduction of melanocytes during larval regeneration. Here we use clonal analysis techniques to develop assays to distinguish roles for these processes during zebrafish larval melanocyte regeneration. We used these clonal assays to investigate which process is affected by the reduction in *kit* signaling. We show that the regeneration defect in *kit* mutants is not due to defects in MSC recruitment or the proliferation, differentiation, or survival of the daughter cells, but is instead due to a defect in stem cell establishment. Our analysis suggests that the *kit* MSC establishment defect results from the inappropriate differentiation of the MSC lineage.

INTRODUCTION

Adult stem cells play crucial roles in the growth, homeostasis, and regeneration of adult tissues. Typically, adult stem cells replace themselves and produce daughters committed to differentiation. Adult stem cells can broadly be classified into 2 categories: stem cells which are continuously dividing, such as the intestinal stem cell (Barker et al., 2007), and those which are largely quiescent but which can be recruited by injury or other physiological need to divide, such as muscle satellite cells (Schultz et al., 1978). The melanocyte stem cell (MSC) falls into the second category of quiescent stem cells (Nishimura et al., 2002). We have developed several methods to activate the MSC in zebrafish including, amputation of the fin in adult fish (Rawls and Johnson, 2000), laser ablation in larvae (Yang et al., 2004), genetic induction in the embryo (Hultman et al., 2009), and drug-induced melanocyte death followed by regeneration in the adult (Chapter 2) and larvae (Yang and Johnson, 2006). Each of these procedures reveals one or more aspect of MSC regulation.

Regeneration output of stem cells can be conceptualized as the product of 1) the number of established stem cells, 2) the percentage of stem cells that are recruited to make differentiating daughters, and 3) the proliferation, differentiation, and survival of these daughter cells. The receptor tyrosine kinase *kit* can play roles in one or more of these processes in many stem cell models including germ cells (Koshimizu et al., 1991; Manova and Bachvarova, 1991) (Sette et al., 2000), hematopoietic stem cells (Li and Johnson, 1994; Valent et al., 1992) (Ashman, 1999), and melanocyte stem cells (Mackenzie et al., 1997; Nishikawa et al., 1991) in mammals. Unlike in germ cells and hematopoietic stem cells, in zebrafish one of the two *kit* orthologs, *kita*, hereafter referred to as *kit*, is only necessary for melanocytes (Parichy et al., 1999). Melanocytes are easily dispensable without affecting viability of zebrafish embryos, easily quantifiable

without requiring additional staining or sacrificing of the animal, and readily ablated (causing regeneration) by both chemical (Yang and Johnson, 2006) and physical means (Yang et al., 2004). During regeneration, new melanocytes incorporate legacy markers such as BrdU, and larvae can be induced to regenerate multiple times (Yang and Johnson, 2006). Together, these data support the notion of an MSC in the larvae that regulates the larval pigment pattern.

Kit is also required for multiples steps in melanocyte development. We have previously isolated a temperature-sensitive mutation in *kit,* kit^{j1e99}, hereafter referred to as kit^{ts} (Rawls and Johnson, 2001). We have successfully used this mutation to demonstrate the temporal requirements for *kit* during adult melanocyte regeneration following fin amputation (Rawls and Johnson, 2001) and larval ontogenetic melanocyte migration and survival (Rawls and Johnson, 2003). In contrast to the temperature-sensitivity of melanocyte regeneration following fin amputation and larval melanocyte migration and survival, kit^{ts} is largely defective for regeneration even at permissive temperatures (Yang and Johnson, 2006). This suggests that larval melanocyte regeneration has a higher requirement for *kit* activity than ontogenetic development or adult regeneration after fin amputation, thus a different technique is required to study the role of *kit* in larval melanocyte regeneration.

Clonal and mosaic analyses can be used fruitfully to study the development of tissues or regeneration of larval or adult tissues. Recently, these methodologies have been used to show the contributions of specific tissue types during complex regeneration events (Gargioli and Slack, 2004; Kragl et al., 2009; Rinkevich et al., 2011; Tu and Johnson, 2011). Additionally, they have been used to elucidate contributions of individual cells within a single tissue during growth, homeostasis, and regeneration (Gupta and Poss, 2012; Snippert et al., 2010; Tryon et al., 2011).

We were interested in determining which of the broadly defined processes discussed above is affected by deficits in *kit* signaling during larval melanocyte regeneration. We developed three assays using clonal analysis to distinguish roles for each of the broadly defined processes. We show that $kit^{null/+}$ heterozygotes are defective for larval melanocyte regeneration, regenerating approximately 50% of the melanocytes as WT. In this genotype, we observed no defects in MSC recruitment or in the proliferation, differentiation, or survival of committed daughter cells. In contrast, our clonal analysis shows $kit^{null/+}$ only establish 54% of the MSCs as WT embryos. Further dissection of this defect with additional clonal analysis suggests that the cells fated to become MSCs differentiate as melanocytes instead.

METHODS

Fish stocks and husbandry

Fish were housed and reared following standard protocols (Westerfield, 2007). All experiments were performed at 28.5°C except for those involving kit^{j1e99}, which were performed at 25°C for which developmental times were adjusted according to Kimmel et al. (1995).

Alleles of kit^{b5} (Parichy et al., 1999) and kit^{j1e99} (Rawls and Johnson, 2001) have been previously described, and will be referred to as kit^{null} and kit^{ts}. WT fish were either the inbred SJA line or *melanophilina* (*mlpha*; Sheets et al., 2007) mutants to facilitate melanocyte counting. *mlpha* mutants contain contracted melanosomes facilitating quantitative analysis, but have no other melanocyte defects. All clonal analysis was performed in *mlpha* or *mlpha; kit*$^{null/+}$ embryos.

Melanocyte Clone Generation

Melanocyte lineage clones labeled with f*Tyrp1*>GFP were generated as previously described (Tu and Johnson, 2010). Briefly, at the 1-2 cell stage embryos were injected with 5-10 pg of a Tol2 plasmid bearing f*Tyrp1*>GFP (Zou et al., 2006) and 5 pg of capped Tol2 transposase mRNA (Kawakami et al., 2004).

To create clones used in Fig. 4, 1-2 cell stage embryos were co-injected with 5-10 pg f*Tyrp1*>GFP transposon, 50 pg of a plasmid with a transposon containing the Xenopus *EF1α* promoter driving RFP expression (*EF1α*>RFP) (Tu and Johnson, 2010), and 5 pg of capped Tol2 transposase mRNA.

Chemical ablation of melanocytes

As previously described (Yang and Johnson, 2006), embryos were treated with 4 ug/mL 4-hydroxyanisole (4-HA, M18655, Sigma Aldrich) to ablate melanocytes either as they developed (1-3 days post fertilization (dpf)) or with a 24-48 hour treatment to ablate fully differentiated melanocytes.

Analysis of clones

Embryos were screened for GFP or RFP clones under an epifluorescence stereomicroscope (Nikon SMZ1500) after being anesthetized with tricaine (methanosulfonate). As we generally generated labeled embryos at rates between 10-40%, we used the Poisson distribution to account for the differential between the number of clones and the number of labeled animals caused by polyclonality in each injection. We used two sample t-tests for comparing clone sizes (Figures 3-2 and 3-5), χ^2 to compare stem cell recruitment (Figure 3-3), and Z-score to compare relative lineage numbers (Figure 3-4 and 3-5).

Recruitment rate calculation

For the recruitment rate of MSCs (Figure 3-3), several models were considered. The simplest model that fit the data was a stochastic model, i.e., that MSCs are chosen randomly and independently in each round. Under this model, the recruitment rate is revealed by consecutive rounds of regeneration. The percentage of first round clones that are also in the second round is the recruitment rate (alternatively, the percentage of second round clones that are also in the first round). Under this model, the probability of not seeing a particular MSC is (1-[recruitment

Table 3-1. Stochastic model predictions for various recruitment rates.

Recruitment rate (%) (rr)	Overlap of 2 rounds (%)[1] rr/(200-rr)	Single round utilization (%)[2] 100/(200-rr)	Unobserved MSCs following 2 rounds (%) (1-rr)^2
10.00	5.26	52.63	81.00
25.00	14.29	57.14	56.25
30.00	17.65	58.82	49.00
40.00	25.00	62.50	36.00
50.00	33.33	66.67	25.00
60.00	42.86	71.43	16.00
70.00	53.85	76.92	9.00
75.00	60.00	80.00	6.25
77.65	63.47	81.73	5.00
80.00	66.67	83.33	4.00
85.00	73.91	86.96	2.25
90.00	81.82	90.91	1.00
95.00	90.48	95.24	0.25
99.00	98.02	99.01	0.01

[1]The overlap between 2 rounds corresponds the dark red circle of Figure 3-3C, D.
[2]The single round utilization corresponds to the dark red circle and the light red (or brown) circles in Figure 3-3C, D.

rate])^2. This model also makes predictions about the overlap between the two rounds of regeneration and the percentage of clones that appear in a given round (Table 3-1).

MSC establishment calculation

For the relative normalized GFP clones (Figure 3-4), the number of GFP and RFP clones was calculated separately using the Poisson distribution to account for the differential of labeled animals and caused by polyclonality for each clutch. The number of adjusted GFP clones was divided by the number of RFP clones to get a normalized GFP clone rate. This normalized clone rate was then used to compare clutches injected in the same experiment to calculate a relative normalized GFP clone rate.

Analysis of ontogeny and regeneration

When analyzing the ontogeny or regeneration of melanocytes in the entire animal, such as in Figure 3-1, 3-10 animals were counted along with WT controls and compared using Student's t-test. Melanocytes in the yolk stripe and over the swim bladder were ignored.

RESULTS AND DISCUSSION

Dosage sensitivity of kit *signaling for regeneration*

Since the $kit^{ts/ts}$ mutant shows an increased requirement for *kit* signaling for larval melanocyte regeneration even at the permissive temperature, we explored the dosage sensitivity of other alleles of *kit*. This increased requirement on *kit* signaling in the larval MSC is similar to the increased requirement of fetal hematopoietic stem cells (HSCs) compared to the requirement of adult HSC to *kit* signaling (Bowie et al., 2007). We checked various other alleles of *kit* as heterozygotes and homozygotes and quantified their larval ontogenetic and regeneration phenotypes (Figure 3-1A). We found genotypes that had normal or nearly normal ontogeny, but had mild to severe regeneration defects (Figure 3-1B). We chose to focus on $kit^{null/+}$ as it had a regeneration defect easily distinguishable from wild type (54% of WT, Figure 3-1B), but still regenerated a significant number of melanocytes (>100/embryo). These data confirm that larval melanocyte regeneration is dosage sensitive for *kit* signaling. Interestingly, these results reveal a haploinsufficiency for *kit* in zebrafish consistent with the haploinsufficiency for *kit* in coat patterns of the mouse (Geissler et al., 1988).

Clonal analysis

Melanocyte regeneration can be divided into 3 broad processes: proliferation, differentiation, and survival of committed daughter cells (Yang et al., 2007); recruitment of the MSC to initially divide and produce committed daughter cells; and establishment of the MSC (Budi et al., 2008; Hultman et al., 2009) (Figure 2A). In order to determine which of these processes contributed to the $kit^{null/+}$ regeneration deficit we used clonal analysis. To study each

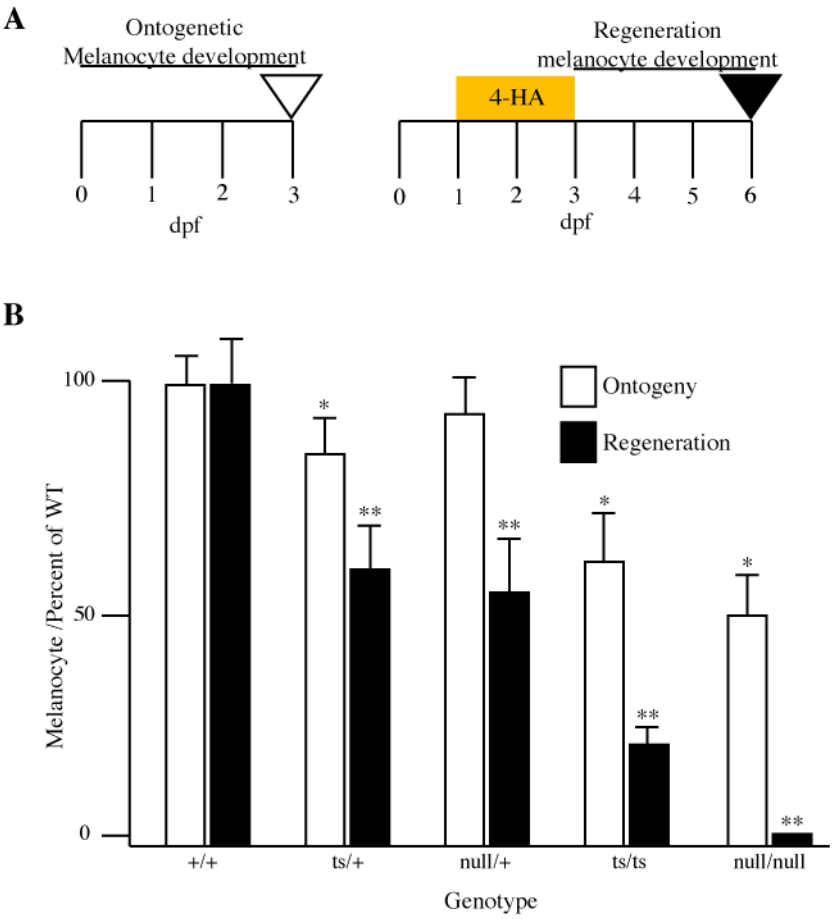

Figure 3-1. Melanocyte regeneration is more sensitive to deficits in *kit* signaling than ontogeny. (A) Schema of the experiments. Fish were reared until 3 dpf and scored for ontogenetic melanocytes (open arrowhead) or treated with 4-HA from 1-3 dpf and scored for regeneration melanocytes at 6 dpf (filled arrowhead). (B) Comparison of *kit* mutant genotypes to WT. 3-10 embryos were compared to WT controls for ontogenetic melanocytes (empty bars) and regeneration melanocytes (filled bars). Experiments with kit^{j1e99} were performed at 25°C, and all others were performed at 28.5°C. Error bars indicate s.d. * indicates $p < 0.05$ ** indicates $p < 0.001$

process we can generate clones by injecting embryos at the 1-2 cell stage with a transposon plasmid containing GFP driven by the *Tyrp1* promoter from fugu (f*Tyrp*1>GFP), which is specifically activated in the melanocyte lineage. Using this protocol, we have shown that transposon integration occurs largely after the midblastula transition, centered on 6 hours post fertilization. This generates melanocyte lineage clones, and we can infer the activity of the MSC and its daughters by analyzing the labeled melanocytes arising during regeneration. Prior to 3 dpf melanocytes arise directly without going through an MSC intermediate (Hultman et al., 2009). We ablate these ontogenetic melanocytes by treatment of embryos with the melanotoxic drug 4-HA from 1-3 dpf. Following washout of 4-HA, melanocytes that regenerate come from MSCs, and those melanocytes that are labeled with GFP are daughters of a labeled MSC.

Proliferation, differentiation, and survival of committed daughter cells are not affected by reduced* kit *signaling.

We first used clonal analysis to analyze the proliferation, differentiation, and survival of MSC daughter lineages by quantifying regeneration clone size (Figure 3-2A). Following injection and melanocyte regeneration (Figure 3-2B), we counted labeled melanocytes in mosaic WT and $kit^{null/+}$ fish after 3 days of regeneration (Fig. 3-2C-D). We then adjusted for potential polyclonality (see Methods). We reasoned that if *kit* function affected the proliferation, differentiation, and/or survival of daughter cells, we would observe smaller clone sizes in the mutant. Instead, we see that regeneration melanocyte clone size is the same for WT (2.9 ± 0.14 melanocytes) and the heterozygous mutant (2.9 ± 0.2 melanocytes) (average ± s.e.m.; Figure 2E). This rules out the model that the reduced regeneration seen when *kit* function is reduced is due to defective proliferation, survival, or differentiation of MSC daughter cells.

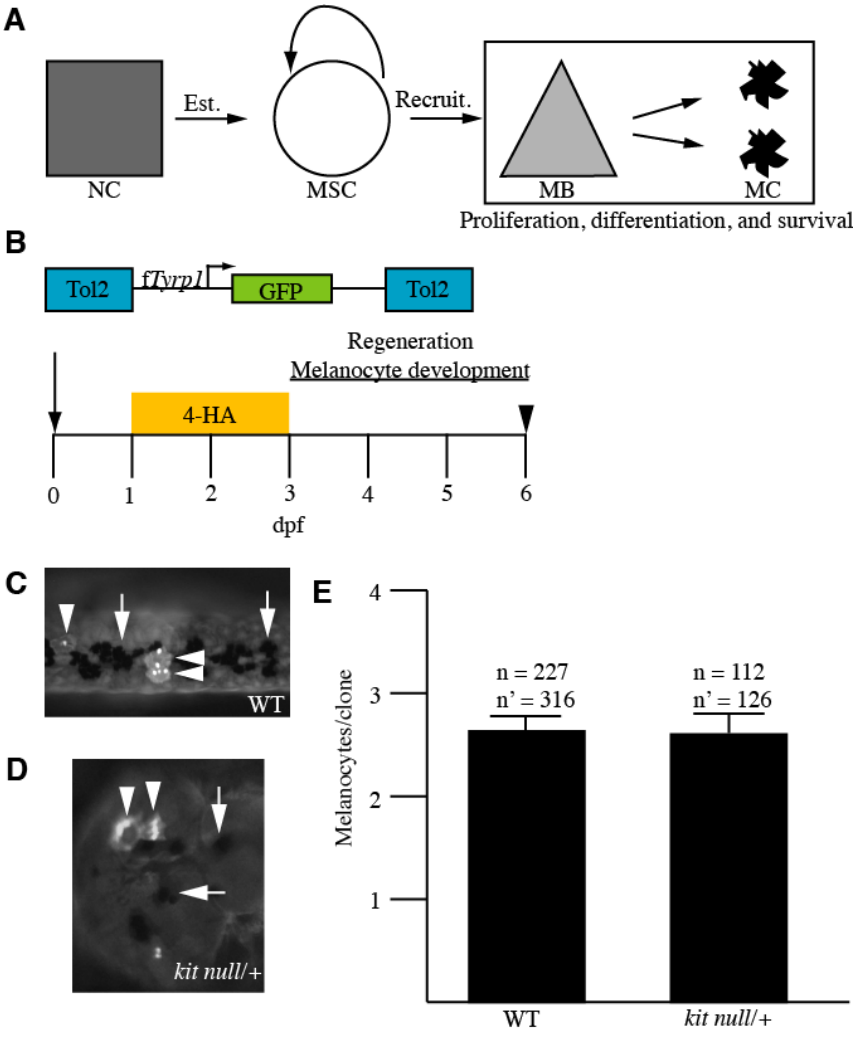

Figure 3-2. MSC daughter cell proliferation, differentiation, and survival are unaffected in *kit*$^{null/+}$ embryos. (A) A general model of melanocyte regeneration. A neural crest progenitor (square, NC) establishes a melanocyte stem cell (circle, MSC) which can be recruited to produce melanoblasts (triangle, MB) which will proliferate and differentiate into melanocytes (MC). Box indicates process tested. (B) Schema of the experiment. Embryos were injected at the 1-2 cell stage (arrow) with transposase and a transposon containing f*Tyrp1*>GFP, treated with 4-HA from 1-3 dpf to ablate ontogenetic melanocytes, and scored for regeneration melanocytes at day 6 (arrowhead). (C, D) Example of clones in WT (C) and *kit*$^{null/+}$ (D) embryos are shown. Melanocytes containing GFP are marked with arrowheads. Some melanocytes lacking GFP are marked with arrows. (E) The average number of melanocytes per clone is the same for both genotypes in regeneration. Reported n values are the number of fish with clones and n' is the adjusted number of clones. Error bars are s.e.m..

Clonal analysis during double regeneration

Our ability to estimate the recruitment rate (Fig. 3-3A) of the MSC is hindered by our inability to observe the MSC directly. We define MSC recruitment rate as the number of MSCs producing melanocytes divided by all available MSCs. The numerator is the number of labeled clones. The denominator requires that we estimate the number of available MSCs. We reasoned that we would need to reveal all or nearly available labeled MSCs by regeneration. For this, we employed clonal analysis using a double (sequential) regeneration assay to assess MSC recruitment rate (Fig. 3-3B). We assumed a model where MSCs were chosen to produce melanocytes stochastically, i.e., MSCs chosen in round 1 were equally likely to be chosen in round 2 (see Methods). This model predicts that to observe >95% MSCs in 2 rounds of regeneration, the overlap between the 2 rounds needs to be > 63.5% (Table 3-1).

First, we examined recruitment in WT mosaic larvae. Of 244 WT embryos injected, 50 contained GFP-labeled regeneration melanocyte clones in the first round. We then challenged these fish to regenerate a second time and re-screened for GFP-labeled melanocytes. Three larvae failed to survive the assay and of the surviving fish that contained GFP-labeled clones after the first round of regeneration, 85% (40/47) regenerated a GFP-labeled clone after the second round of regeneration. Of the 181 surviving fish that did not contain a GFP-labeled clone after the first round of regeneration, 9 regenerated GFP-labeled clones after the second round of regeneration. Thus, we observed 59 total clones, with 50 (85%) revealed in the first round and 49 (83%) revealed in the second round (Figure 3C). As not all larvae containing clones survived the assay, the second round recruitment rate is slightly underestimated and the first round recruitment rate is slightly overestimated. These stem cell recruitment rates predict very few, if any, available MSC lineages failed to contribute to one or the other round of regeneration. These results also show that the MSC recruitment rate is 83-85%.

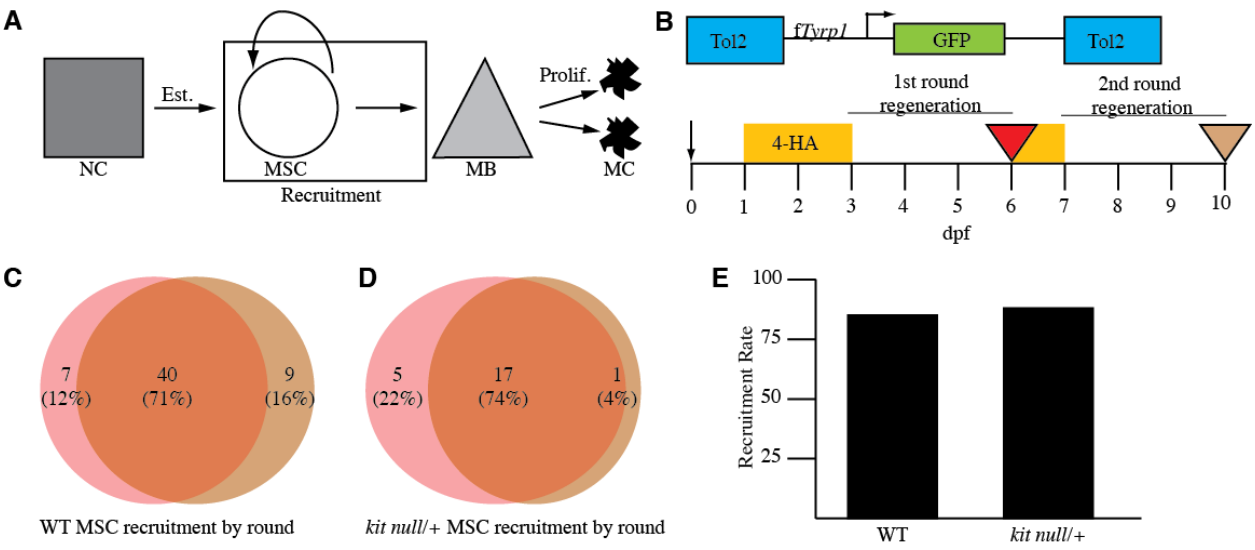

Figure 3-3. MSC recruitment is unaffected in *kit*$^{null/+}$ embryos. As in Figure 2, (A) represents a general model for melanocyte regeneration. Box indicates process tested. (B) Schema of the experiment. Embryos were injected at the 1-2 cell stage (arrow) with transposase and a transposon containing f*Tyrp1*>GFP, treated with 4-HA from 1-3 dpf, scored for regeneration melanocytes at day 6 (red shaded arrowhead), treated again with 4-HA from 6-7 dpf, and scored for regeneration again (brown shaded arrowhead). (C,D) MSC recruitment rates for WT (C) and *kit*$^{null/+}$ (D). The number of embryos (and percentage) containing a GFP clone in the first round only (light red), both rounds (dark red), and second round only (brown) are not significantly different between the genotypes ($\chi^2 = 3.35$, d.f. = 2, $p > 0.1$). (E) Recruitment rate is not different between WT and *kit*$^{null/+}$ embryos.

The high degree of overlap (>70%) between the two rounds allow us to confidently believe that nearly all available MSCs contributed to the two subsequent rounds of regeneration. It was possible that if only a minority of MSCs were recruited in each round that we could not expect to see all MSCs across the two sequential rounds. Having now determined a baseline MSC recruitment rate, further studies can analyze other characteristics of MSC recruitment, including the effects of drugs or environmental factors that effect MSC recruitment, or the roles of genes in recruitment rate (below).

We then looked at MSC recruitment in $kit^{null/+}$ mosaic larvae. WT recruitment rates are approximately 80%, and the $kit^{null/+}$ larvae regenerate 53% of the melanocytes of WT. If *kit* was involved in recruitment of MSCs, we would expect to see for each round of regeneration the recruitment rate drop to approximately 44% (53% of 83% is 44%). This would also be evident by a large decrease in the expected overlap between the 2 rounds (Table 3-1). We injected 127 $kit^{null/+}$ fish of which 22 contained melanocyte clones in the first round of regeneration. Of these fish, 77% (17/22) regenerated a GFP-labeled clone after the second round of regeneration. Of the 89 surviving fish that were not GFP-labeled after the first round of regeneration, 1 regenerated a GFP-labeled clone after the second round of regeneration. Thus, we observed 23 total clones, with 22 (96%) recruited in the first round and 18 (78%) recruited in the second round (Figure 3D). Thus, the recruitment rate for $kit^{null/+}$ is 78-96%. These recruitment rates are not significantly different from those observed in WT ($\chi^2 = 3.35$, d.f. = 2, $p>0.1$), and fail to account for the 46% reduction of regeneration melanocytes seen in $kit^{null/+}$ fish. Thus, we conclude that *kit* causes no deficit in recruitment of the MSC.

Some ambiguity is possible in this analysis. If the daughter cells of the MSC died before they had a chance to divide, by our assay this would appear as a defect in recruitment, rather than

proliferation, differentiation or survival. In this case, where *kit*$^{null/+}$ shows no defect in either MSC recruitment or proliferation, differentiation, or survival of the daughter cells, we can confidently conclude that neither process is affected.

Although the adult stem cell in some systems, such as the intestinal stem cell (Barker et al., 2007), is constitutively active, the MSC is usually quiescent (Hultman and Johnson, 2010; Nishimura et al., 2002). Although quiescent stem cells can be put through multiple injurious events to cause multiple rounds of regeneration, observing the individual rounds often requires the sacrifice of the animal or other laborious means to score. This has left open the question of how many stem cells contribute to a single regenerative event. A thorough understanding of this question may be important to tune endogenous adult stem cells that are artificially activated. We find that most, approximately 80%, but not all MSCs respond during any given regenerative event. As far as we are aware, this is the first quantitative analysis of quiescent stem cell activation.

MSC establishment is reduced in* kit *mutants

Having excluded roles for MSC recruitment and daughter cell proliferation, differentiation, and survival, we lastly tested the model that *kit* mutants reduce the establishment of the MSC (Figure 4A). This model predicts that there will be fewer lineages used to produce the MSCs in the *kit*$^{null/+}$ embryos. This model would be easy to test if we could visualize and quantify the MSC directly. Being unable to visualize the MSC directly, we reasoned that we could detect a deficit in MSCs by comparing the rates of labeling regeneration melanocytes in kit heterozygotes and WT embryos. In 3 independent sets of injections, we found the proportion of

kit$^{null/+}$-to-WT GFP-labeled larvae was 0.40, 0.63, and 0.69 (0.57 ± 0.15). These results support that *kit* signaling affects MSC establishment.

Directly using the rate of GFP-labeled regeneration melanocyte clones ignores alternative explanations. One is the experiment-to-experiment variability in labeling efficiency, which our experience suggests is as much as two-fold (not shown). Additionally, there remains the possibility that the *kit*$^{null/+}$ stocks have an independent deficit in transposon integration. To control for these possibilities, we co-injected RFP driven by the constitutive promoter *ef1α* (Figure 3-4B). This promoter is expressed in all cell types, thus every integration event will be observed. We were then able to normalize the number of GFP clones with the number of RFP labeled embryos. We performed this experiment three times, and found the normalized proportion of *kit*$^{null/+}$ to WT GFP clones was 0.58, 0.37, and 0.68 (0.54 ± 0.16, $p < 0.01$; Figure 3-4C). The MSC establishment deficit is the same as that seen for the *kit*$^{null/+}$ melanocyte regeneration defect, suggesting it explains all of the regeneration defect. Therefore, we conclude that *kit* functions in larval melanocyte regeneration to establish the MSC, but that *kit*$^{null/+}$ does not affect recruitment or proliferation, differentiation, or survival of the daughters of the MSC.

The finding that *kit* signaling is important for MSC establishment was unexpected. Although *kit* has been shown to be important for stem cell establishment in other systems (Manova and Bachvarova, 1991), we had previously shown that *kit* signaling was not involved in the establishment of a different MSC population used in adult fin regeneration, but is involved in the recruitment and/or proliferation, differentiation, or survival of the daughter cells. This was demonstrated by rearing *kit*$^{ts/ts}$ at the restrictive temperature from larval stages, downshifting only after fin amputation. These fish regenerated normally, whereas reciprocal shifts failed to regenerate normally. (Rawls and Johnson, 2001). We did not find any evidence in our clonal

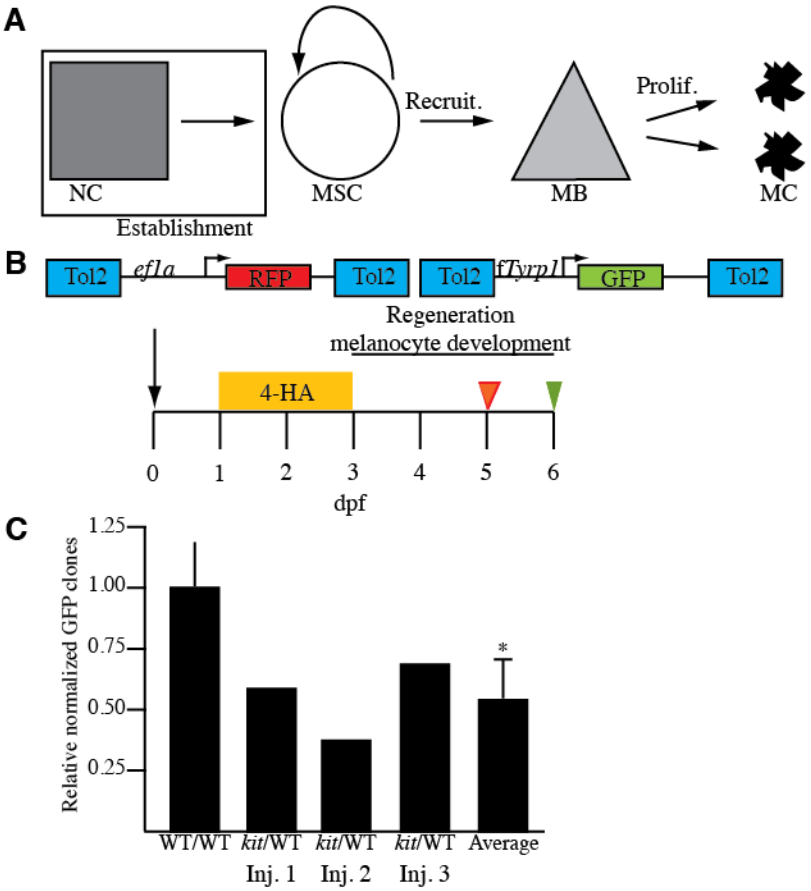

Figure 3-4. MSC establishment is reduced in $kit^{null/+}$ embryos. As in Figure 2, (A) represents a general model for melanocyte regeneration. Box indicates process tested. (B) Schema of the experiment. Embryos were injected at the 1-2 cell stage (arrow) with transposase, a transposon containing *ef1α*>RFP, and a transposon containing f*Tyrp1*>GFP, treated with 4-HA from 1-3 dpf, scored for RFP at 5 dpf (red arrowhead), and scored for GFP at 6 dpf (green arrowhead). (C) Bar graph showing the relative normalized clone rate (see Methods). The first bar shows a comparison of 2 sets of injections in WT embryos, with the line showing the deviation from expected (1.0). Bars 2-4 show independent experiments comparing the normalized integration rates of $kit^{null/+}$ and WT. Bar 5 shows the average and s.d. (0.54 ± 0.16) of bars 2-4. This relative normalized rate of 0.54 is identical to the residual melanocyte deficit in $kit^{null/+}$ embryos. * indicates $p < 0.01$.

analyses suggesting a role for *kit* in larval MSC recruitment or daughter cell proliferation, survival, or differentiation. Thus, *kit* performs different functions in each of the different melanocyte lineages that require *kit*. This emphasizes the folly of pigeonholing a gene's function from only one of its requirements in the organism.

We used these clonal analyses to show a role for *kit* in MSC establishment. We note that our analysis here is limited to the dosage sensitive, or haploinsufficient roles for *kit* in melanocyte regeneration. These assays clearly show the role of *kit* in establishing the MSC, but we cannot use them to exclude an effect of complete lose of *kit* signaling on MSC recruitment or daughter cell proliferation, differentiation or survival.

The role of* kit *signaling in MSC fate determination

Having shown that *kit* is required for MSC establishment, we next asked what mechanism was perturbed. We have previously shown that all lineages that contain an MSC likely come from a neural crest precursor that will also produce an ontogenetic melanocyte lineage (Figure 3-5A; Tryon et al., 2011). Based on this model, we could imagine three possible ways to disrupt MSC establishment: (1) death of the neural crest precursor (Figure 3-5B), (2) death of the MSC (Figure 3-5C), or (3) differentiation of the cell normally fated to become the MSC (Figure 5D). Each of these models makes a different prediction of the number of ontogenetic melanocyte lineages and ontogenetic melanocyte clone size (Figure 3-5B-D), explained in more detail below.

The MSC lineage and the directly developing ontogenetic lineage segregate at approximately the same time as the occurrence of transposon integration. This means that integration events can happen before the fate segregation, generating both lineages (bipotential labelings), or after fate segregation, labeling only a single lineage. We had shown previously

that approximately 60% of clones were bipotential, and the remainder generated only ontogenetic melanocytes or regeneration melanocytes (Tryon et al., 2011). Under Model 1 (Fig. 3-5B), where some neural crest progenitors are killed in the mutants, we would expect to find similar ratios of clone classes in WT and mutant embryos. In contrast, Models 2 (Fig. 3-5C) and 3 (Fig. 3-5D) predict fewer bipotential and regeneration-only clones. We followed the established methods of Tryon et al. (2011) to test whether there were differences in the ratios of clone classes produced by $kit^{null/+}$. We found a significantly reduced rate of larvae containing bipotential clones of the clones that contained an ontogeny clone in the mutant (WT – 19/44, $kit^{null/+}$ - 12/71, $p<0.005$, Fig 5E). This result rules out Model 1, but is consistent with Models 2 and 3.

To distinguish between the remaining models, we again turned to clonal analysis. As the $kit^{null/+}$ mutant has nearly the same number of ontogenetic melanocytes as WT (266 ± 20 melanocytes for WT, 249 ± 22 melanocytes for $kit^{null/+}$, $p > 0.1$; Fig. 5F)., we reasoned that a change in the number of ontogenetic lineages should be reflected by a change in the number of ontogenetic melanocytes per lineage (clone size). Under Model 2, the death of the MSC should leave the ontogenetic clone size unaffected, as the number of ontogenetic lineages is unchanged (Figure 3-5C). Under Model 3, direct differentiation of the presumptive MSC precursor into melanocyte(s) should lead to a decrease in average ontogenetic clone size as the number of ontogenetic lineages has increased (Figure 3-5D), with no corresponding change in the total number of differentiated melanocytes (Figure 3-5F).

We injected f*Tyrp1*>GFP at the 1-2 cell stage and screened for ontogenetic clones at 3 dpf. The clone size for WT embryos, 3.7 ± 0.3 melanocytes, is significantly larger than the clone size in $kit^{null/+}$ embryos, 3.0 ± 0.2 melanocytes (average ± s.e.m., $p<0.05$, Figure 3-5G). This

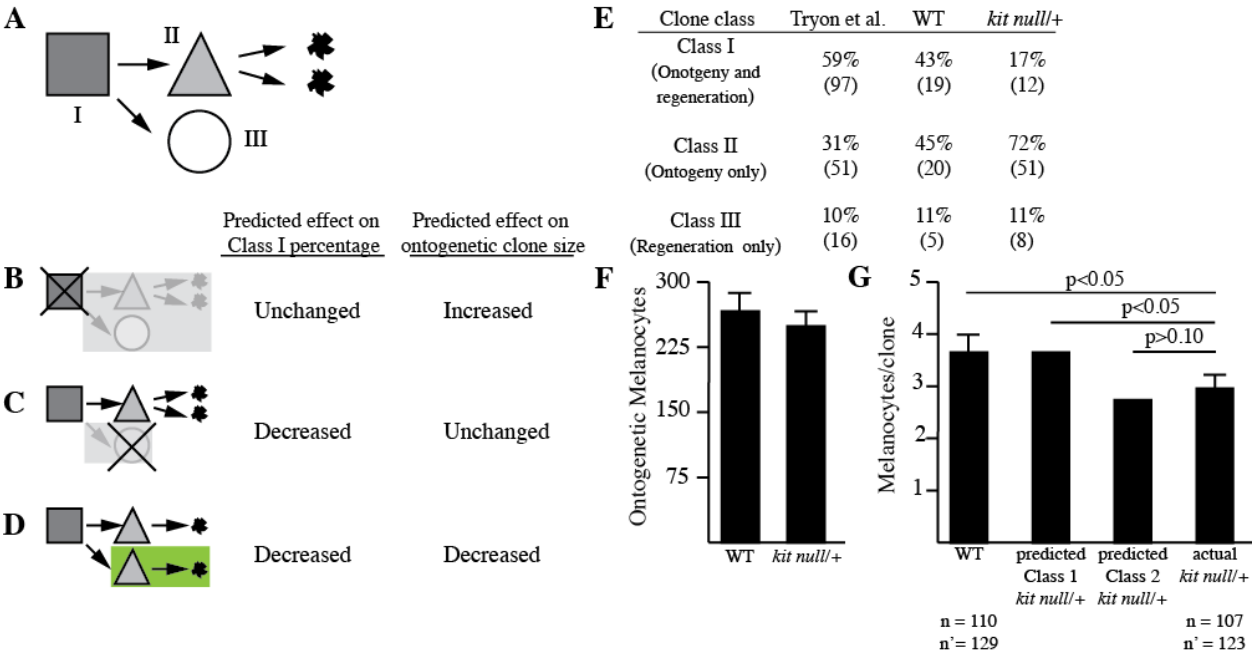

Figure 3-5. Reduction of *kit* signaling leads to an increase in ontogenetic melanocyte lineages. (A) A neural crest progenitor cell (square) produces an MSC (circle) and a melanoblast (triangle) followed by melanocyte differentiation. Roman numerals indicate clone classes caused by varying times of transposon integration. (B-D) Possible models explaining the effect of *kit* deficit on MSC establishment. Models include the predicted effect of *kit* deficit for each model on Class I clone percentage and ontogenetic melanocyte clone size. Cell death in (B,C) is represented by "X," and fainted pathways indicate consequence of cell death. Green shaded box in (D) indicates inappropriate differentiation of MSC (E) Effect of $kit^{null/+}$ on generation of different clone classes. Shown is data from Tryon et al. (first column; 2011), WT data from this study (second column), and $kit^{null/+}$ (third column). The percentage of each clone class is shown, as well as the unadjusted number of clones in parentheses. WT data from this study is not significantly different from that generated by Tryon et al. ($\chi^2 = 4.9$, d.f. = 2, $p > 0.05$). Clone class distribution in $kit^{null/+}$ is significantly different ($\chi^2 = 59$, d.f. = 2, $p < 0.001$). The difference is due to a reduction in ontogeny and regeneration clones co-occurring (Class I) (Z-score = 3.1, $p<0.005$) (F) The number of ontogenetic melanocytes is not significantly different between WT and $kit^{null/+}$. (G) The average number of ontogenetic clones is smaller for $kit^{null/+}$ than in WT, indicating an increase in the number of lineages of ontogenetic melanocytes. Bars 2 and 3 are predictions if 100% of integrations were class I and II, respectively. Both integration events are possible (see text). Error bars are s.e.m. Reported n value is the number of fish with clones, and n' is the number of adjusted clones.

result is inconsistent with Model 2, but consistent with Model 3. Therefore, we conclude that cells normally fated as MSCs instead differentiate into ontogenetic melanocyte lineages when *kit* signaling is reduced.

It remains unclear when this inappropriate differentiation of cells normally fated to become MSCs take place. Signaling from *kit* could be required as early as the segregation of the MSC lineage from the directly developing ontogenetic lineage (~6 hours post fertilization). However, we first observe *kit* expression in neural crest cells between 14-18 hours (Parichy et al, 1999), suggesting a role for *kit* in migration of the presumptive MSC from the neural crest, or in taking up its position in a yet to be identified niche. Our data now sets the stage for addressing this question.

Conclusion

We took advantage of the dosage-sensitivity of melanocyte regeneration for kit function to explore the role of kit signaling in MSC regulation. We developed clonal analysis methods that allowed us to show that the melanocyte regeneration deficit observed in $kit^{null/+}$ is a defect in establishing the MSC, rather than recruiting the MSC to generate new melanocytes, or in the proliferation, differentiation, or survival of the MSC daughters. Clonal analysis also suggests that lacking sufficient kit signaling, cells destined to become MSCs instead directly differentiate as melanocytes. Clonal analysis methods developed in this chapter can be used to study other defects in larval melanocyte regeneration, or regulation of other adult stem cells.

ACKNOWLEDGEMENTS

Brian Stevens, Rachel Kirchstetter, and others provided fish facility support. We are especially grateful to Rob Tryon and Shu Tu for feedback on clonal analysis methods. This work was supported by NIH grant GM05698 (to SLJ).

Chapter 4

A quantitative estimate of spermatagonia in mutagenized zebrafish males.

INTRODUCTION

Efficient induction of point mutants is a critical first step in genetic analysis. In zebrafish, treatment of adult males with ENU has been the principal method of choice for performing mutant screens. The advantages of performing mutagenesis on adult males are several: robust protocols exist; they can be bred naturally or via in vitro fertilization, producing 100s of embryos in a single cross; and each male can be reused to produce thousands of mutagenized genomes over their life time.

Despite this common usage of adult male ENU mutagenesis, it remains unclear how many spermatagonia per male are targets of the mutagenesis and contribute mutagenized gametes. This number will provide guidance on how many mutagenized gametes can be sampled from each mutagenized male with a reasonable assurance that each isolated mutation is independent. For instance, if one could mutagenize an infinite number of males, and sample a single gamete from each, there would be no risk of non-independent mutations. Although this is close to the practice in *C. elegans* screens (Jorgensen and Mango, 2002), this is rarely practical in zebrafish for several reasons: mutagenizing a large number of males is difficult; males often comprise less than half of any stock; and, inevitably, some fish die during the mutagenesis. As a consequence, many gametes are used from each mutagenized male (Driever et al., 1996; Haffter et al., 1996; Mullins et al., 1994; Rawls et al., 2003; Rawls and Johnson, 2001; Yang et al., 2007). This is not a problem if there are many spermatagonia. If the number of spermatagonia is finite (<1,000), than the probability of redundant sampling becomes significant in many applications.

In this chapter, we establish a lower bound on the number of spermatagonia in

mutagenized males. We performed mutagenesis on a group of males and screened them for mutations at 2 loci, *albino* and *kit*. We showed that the mutation rates for mutagenized males harboring mutations do not have a significantly higher mutant load than a mutagenized male chosen randomly. We then used some conservative assumptions to estimate the lower bound of spermatagonia per mutagenized male is approximately 450 (95% CI 335-652) spermatagonia per mutagenized male.

METHODS

Fish stocks and maintenance

Fish stocks were maintained and reared according to standard protocols. Adult inbred sjD males (Rawls et al., 2003) were used for mutagenesis (below) and then crossed to *albino*^{b4} (Streisinger et al., 1986) to test for *albino* non-complementation and/or *kit*^{b5} (Streisinger et al., 1986), *kit*^{j1e99} (Rawls and Johnson, 2001), and/or *kit*^{j1e78} (Rawls and Johnson, 2003) to test for *kit* non-complementation.

Mutagenesis

ENU mutagenesis was performed as previously described (Mullins et al., 1994; Solnica-Krezel et al., 1994). A 1.0 g isopack of ethylnitrosourea (ENU, Sigma, N3385) was dissolved into 60 mLs of a 0.1 mM phosphate, 0.05mM citrate, and 10% ethanol ph5 solution. 12.5 mls was added to 550 mls system water with 0.1 mM phosphate, ph 6.5 and 0.01mg/ml tricaine to make a 3 mM ENU solution. The mutagen solution was held at 21- 22^{o}C. 20 young (~ 3 months) SJD males were transferred from a similar volume of 0.01 mg/ml tricaine to the mutagen solution. Fish were transferred using mesh-bottomed breeding cages and mutagenesis was performed in dark, to further minimize stress during and after mutagenesis. After 1 hour in mutagen, fish were transferred to a fresh volume of system water with 0.05 mM phosphate (no tricaine) and allowed to recover for 2 hours, then transferred to clean system water and left in the dark overnight. The next day, fish were washed through a further 2 volumes of system water, then returned to their aquaria for normal husbandry. This protocol was repeated weekly for a total of 5 treatments. 2-3 weeks after the last treatment, sperm was harvested and discarded, and

after a further 2-3 weeks, mutagenized males were bred to albino and sparse testers to assess mutation rates.

Statistics

To estimate the number of spermatagonia per male, we assumed that there was random sampling from a finite number of spermatagonia per mutagenized male. We assumed only a single locus would be responsible for non-complementation and that only a single *albino*, or, similarly for *kit,* mutation was induced in the germline of each mutagenized male. (Increasing the number of mutations per mutagenized male increases the number of spermatagonia per mutagenized male, but this assumption establishes a lowest bound.) We then employed the binomial probability mass function to produce an estimate and the binomial cumulative distribution function to produce the confidence intervals.

To estimate the number of genomes screened, we utilized a Poisson distribution to

$$P(X = k) = \frac{\lambda^k e^{-\lambda}}{k!}$$

estimate how many genomes remained unscreened. We set lambda equal to (genomes screened)/(2*spermatagonia per male [as determined above]) and k = 0, to get the percentage of unscreened genomes (which is also the probability that the next genome screened is a heretofore unscreened genome). We multiplied that number by twice the number of spermatagonia per male to get the number of unscreened gametes, and subtracted that number from twice the number of spermatagonia per male to get the number of screened gametes.

RESULTS

To provide some bounds on the effective number of mutagenized spermatagonia per male, we subjected adult wt males to standard ENU mutagenesis protocols (see methods). First, 3 month old SJD males were squeezed to identify males that were producing sperm (>90% of males produced sperm), and 80 of these were subjected to 5 weekly rounds of exposure to 3 mM ENU (see methods). Mutagenesis was terminated after 5 rounds because fish were looking stressed and some males were dying during the intervening weekly recovery periods. Following the last ENU treatment fish were then allowed 2-3 weeks to recover from the mutagenesis, with a single squeezing to help clear gametes that were post-meiotic at the time of mutagenesis. We then used in vitro fertilization procedures to cross each of 36 surviving males to albino or kit testers. Consistent with the notion that all sperm at this time were derived from spermatagonia rather than post-meiotic sperm, we found no mosaic *albino* expression in the pigmented retinal epithelium (Chakrabati et al., 1983). The results of our initial assay for mutation rate are shown in Table 1. These experiments revealed an average rate of 0.00101 albino and 0.00096 kit mutations per gamete. These rates are consistent with mutagenesis rates reported in other studies as well as from this lab (Rawls and Johnson, 2001), except typically we expect to find a higher mutation rate at kit than at albino.

The number of spermatagonia can not be accurately calculated directly from the population mutation rate because the mutation rate of the population is dependent on the number of spermatagonia per mutagenized male and the mutation load of each male. A very small number of spermatagonia per mutagenized male will lead to few males having mutations, but those males producing mutant offspring very frequently. A variable mutation load may lead to

males harboring a mutation at one locus being much more likely to harbor mutations at other loci. Rescreening individual males harboring mutations and comparing the individual rates to the population rates can control for these variables.

One variable affecting the mutation rate is the mutation load that each male bears. If a variable mutation load was an issue, than mutagenized males found to harbor a mutation at one locus would be expected to show a higher incidence of mutation at other loci. It would also imply that the mutations generated were more likely to spontaneous than directed (Luria and Delbrück, 1943). There was not enough overlap in the initial screen (12 males harbored at least one mutation) to provide enough power to answer this question. To address this, we rescreened males that had produced *kit* embryos for mutations at the *albino* locus. We did not include the 2 males that produced both alb^- and kit^- embryos in the initial screen. We found 0.0013 (5/1787) mutations per gamete at the *albino* locus in these males that had previously been shown to have a mutation at the *kit* locus, but not at the *albino* locus (Table 1). This is not significantly different (Z-score = 1.9, $p>0.05$) than the population average. Additionally, we did the inverse set of crosses and rescreened the males that had produced *albino* embryos for mutations at the *kit* locus. We found 0.00051 (2/3741) mutations per gamete at the *kit* locus in these males that had previously been shown to have a mutation at the *albino* locus but not at the *kit* locus (Table 1). This is not significantly different (Z-score = 0.78, $p>0.1$) than the population average. This demonstrates that the males that had one germline mutation on the initial screen are not bearing a significantly higher mutation load than the male pool at large.

Another variable affecting mutation rate is the size of the germline. If males have only 50 spermatagonia per male, we would expect to see an approximately 10 fold increase in mutations/gamete over the initial screen. Alternatively, if males have extremely large germlines,

Table 4-1. Estimation of SSCs from mutation rate

Population tested	Locus tested	No. males	Mutant embryos	Screened embryos	Mutations per gamete	Estimated SSCs (95% CI)
General	*kit*	22	7	7326	9.6×10^{-4}	523 (254-1060)
General	*alb*	26	9	8875	1.01×10^{-3}	493 (260-925)
kit harborers[1]	*kit*	5	6	3843	1.6×10^{-3}	320 (147-680)
kit harborers[1,2]	*alb*	3	5	1787	2.8×10^{-3}	179 (77-405)
alb harborers[1,2]	*kit*	4	2	3741	5.1×10^{-4}	935 (259-3023)
alb harborers [1]	*alb*	6	1	3526	2.8×10^{-4}	1763 (317-7275)
Total	*kit*	26	15	14910	1.0×10^{-3}	497 (304-815)
Total	*alb*	29	15	14188	1.06×10^{-3}	473 (287-775)
Total	*kit* + *alb*	36	30	29098	1.03×10^{-3}	485 (340-691)

SSC = Spermatagonial Stem Cell

[1] These numbers are for the rescreen only. They do not include the original screen.

[2] These numbers do not include 2 males that were positive for both loci in the initial screen.

we might not see any replication from the original screen. To explore the number of spermatagonia in mutagenized males, we rescreened the males that produced *kit* and *albino* offspring to see if the number of spermatagonia per mutagenized male was significantly different than the population at large. At the *kit* locus, we rescreened the 5 males that produced mutant offspring in the initial screen. In the rescreen, 3 of the 5 males gave at least 1 additional mutant embryo when screened (>500 embryos tested/male). The mutation rate for the rescreen was 0.0016 (6/3843) *kit* mutations per gamete, which is not significantly different from the population at large (Z-score = 0.892, p >0.1). We also rescreened the 6 males that produced *albino* offspring in the initial screen. In the rescreen, 1 of these males produced an additional mutant embryo (>500 embryos/male). The mutation rate for the rescreen was 0.00028 (1/3526), which is not significantly different than the population at large (Z-score = 1.29, p>0.1) (Table 1). Therefore, it does not seem to be the case that mutagenized males have a small number of spermatagonia.

We used these mutation rates to produce an estimate of the number of spermatagonia per male. As none of the subsets of data appeared statistically different from each other, we combined all the groups. We assumed that each germline contained one mutation and that spermatagonia were finite and chosen at random. We estimate there are approximately 485 spermatagonia per mutagenized male (95% CI 340-691) (Table 1). Retesting males also allowed us to look at the mutation rates for individual males. If we assume that most or all of the males harbor only a single mutation in their germline, then sufficient resampling should produce a mutation rate in line with the number of genomes in the germline. Most of the mutagenized males showed a mutation rate of approximately 0.001 (9/14 were between 0.0005 and 0.002, Figure 1), consistent with approximately 500 spermatagonia.

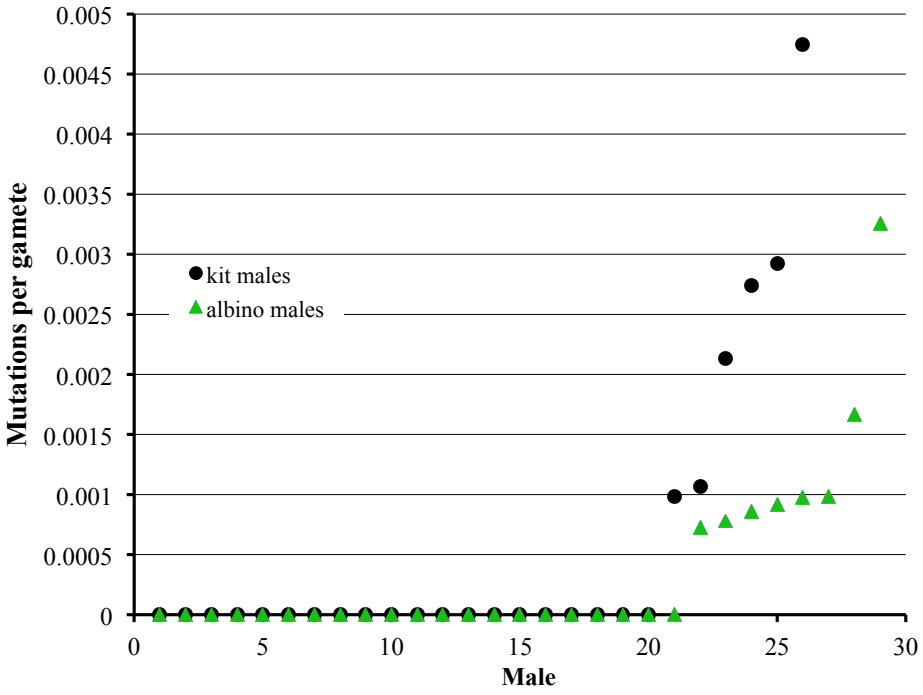

Figure 4-1. Mutational rates for individual mutagenized males at two loci. Most mutation rates (8/14) are close to the predicted mutation rate for 485 spermatagonial stem cells (0.0010). Males are numbered individually for each locus, and may not have been screened at both loci. The total number of males tested is 36.

DISCUSSION

In order to make efficient use of mutagenized zebrafish males, we first need an estimation of the number of spermatagonial stem cells (spermatagonia per male). We screened for non-complementation of 2 loci from mutagenized males, and found 30 mutants in 29,098 embryos. We showed that germline size was similar in all males, as was the mutation load. We then used these numbers to estimate 485 spermatagonia per mutagenized male.

Our estimate is a lower bound and comes with several caveats. The mutagenesis process may kill spermatagonia, giving fewer mutagenized spermatagonia than spermatagonia that were originally present (although this is immaterial for understanding the number of mutagenized spermatagonia). We assumed each male harbored a single mutation per locus. The fish we were using is that the fish were young (only 2-3 months old). Fish continue to grow isometrically as they age (Goldsmith et al., 2006; Iovine and Johnson, 2000), so it is reasonable to presume the germline may also add stem cells. The inbred sJD line used tends to have smaller males than other lines, and thus may have a smaller germline than other lines.

Superficially, our estimate seems reasonable. We have often found mutation rates of approximately 0.001, which would suggest approximately 500 spermatagonia. Additionally, mice have approximately 35,000 spermatagonia per male (Tegelenbosch and de Rooij, 1993), which is approximately 1,300 spermatagonia/g body weight. Our estimate leads to approximately 1,600 spermatagonia/g body weight.

Our estimate may appear to depend on the efficacy of the mutagenesis performed on the males screened. Indeed, if the only measure was the rate of the population at large, then this

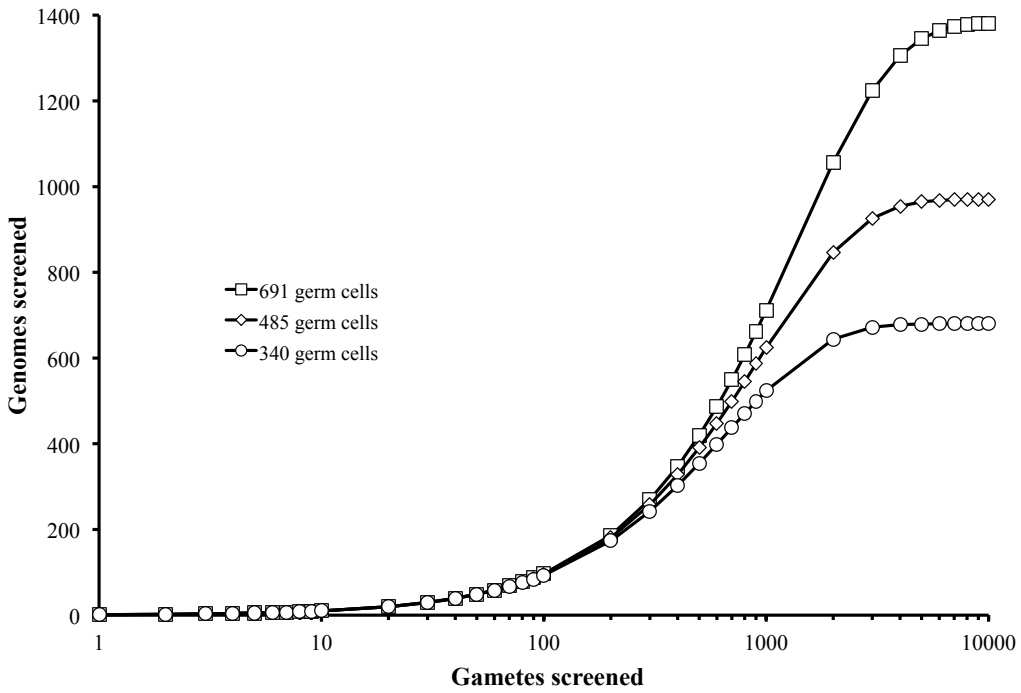

Figure 4-2. Number of independent genomes screened as a function of gametes screened. The graph depicts the number of independent genomes screened from a single mutagenized male compared to the number of gametes screened by that male. The numbers of germ cells chosen for depiction are the average and 95% confidence intervals (see text).

would undeniably be the case. Rescreening the males that initially harbored mutations, however, controls for this. Ideally, we would have screened 5,000-10,000 gametes per mutagenized male, rather than the ~1,000 actually preformed. This would give us a more accurate estimate of the mutation rate in these males, and coupled with the assumption of one mutation per mutagenized germline would reveal the size of the germline. Since the unbiased screen and the selected rescreen gave the same mutation rate, we feel confident that our estimate is not heavily dependent on the efficacy of the mutagenesis.

While we obviously can't describe a one-size-fits-all mutant screen, we can use these new estimates to determine important factors for when to stop sampling from individual males, such as how many of the gametes already screened are likely to be independent (Figure 4-2) and the percentage of gametes left that are unsampled (Figure 4-3). For instance, if you need 300 independent genomes from each male, you will need to screen 340-400 genomes from each male. If you want to stop when you reach a 20% redundant sampling rate (a 20% chance that the next genome has already been seen), then you should screen only 150-300 genomes from each male.

We can also use these estimates to assess the likely number of genomes screened in large screens. Haffter et al. performed a large F3 screen (Haffter et al., 1996). A typical F3 screen to reveal heterozygous mutations is more severely limited by the number of families that can be generated, and might typically screen from 500 to 4000 mutagenized gametes. Haffter et al. estimated that they had screened 3857 independent mutagenized genomes, achieved this by generating 49 mutagenized males, and limiting their sampling to an average of sampling approximately 126 gametes per mutagenized male. We would estimate that they had 4.4-8.7% redundant sampling, leaving 3520-3686 independent gametes.

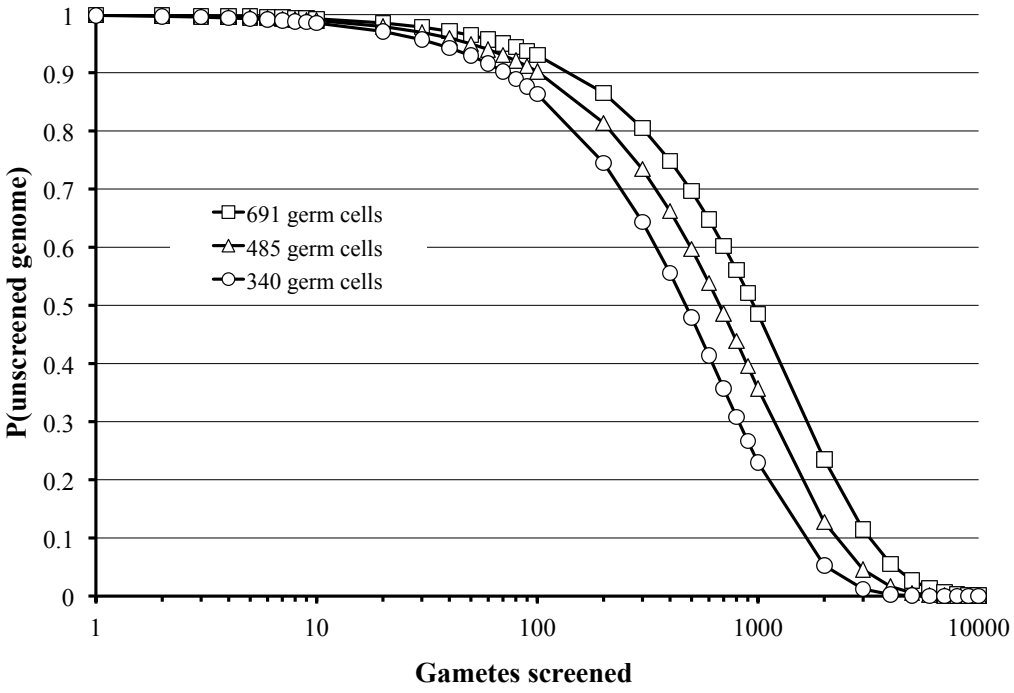

Figure 4-3. The probability of the next genome being novel as a function of gametes screened. The graph depicts the probability that the next genome screened from a mutagenized male is a new genome from that mutagenized male compared to the number of gametes screened from that mutagenized male. This is the same as the percentage of gametes not seen in a mutagenized male with the number of gametes screened. The number of germ cells depicted is the average and 95% confidence interval (see text).

Rawls and Johnson took the approach that there were a very large number of spermatagonia in their non-complementation screen (Rawls and Johnson, 2001). They screened 83,000 gametes from 45 males (>1,800 gametes/male). We would estimate that of the genomes sampled 45-65% were redundant, leaving only 28,600-45,900 independent gametes. This screen yielded 247 non-complementing mutants, some of which can reasonably expected to not be independent. Only 10 were sequenced (Rawls and Johnson, 2001) (and 3/17 in a very specific class (Rawls and Johnson, 2003)) and did not yield any duplicate mutations. However, this sample is too small to be conclusive.

Another issue that we did not address is the possibility of germline replacement. That is, a pool of spermatagonia produces the sperm that was utilized during our screen, and another, perhaps small, pool of spermatagonia was left in reserve to replace the "active" spermatagonia. If this were true, breeding the same male over the course of weeks or months may result in different mutation rates.

ACKNOWLEDGEMENTS

We thank Ryan McAdow for technical assistance with these experiments. We also thank Francesco Vallania for discussions of statistics.

CONCLUSIONS

In this thesis, I developed several tools to help dissect melanocyte stem cell (MSC) functions, and solve some of questions in the field. In Chapter 2, I developed a drug, neocuproine, that can ablate melanocytes specifically and only in the adult. Previously, adult melanocyte regeneration could only be accomplished through fin amputation, which led to a complex regeneration event. In Chapter 3, I developed a series of assays that quantitatively can detect perturbations in MSC establishment, MSC recruitment, and/or the proliferation, differentiation, and survival of MSC daughter cells. Using these assays, I was able to discover that *kit* signaling was essential in MSC establishment, specifically for preventing the presumptive MSC from differentiating and contributing to the ontogenetic pigment pattern. Additionally, these assays solved an important question for regenerative medicine: how many endogenous stem cells are activated during a regenerative event? As far as I can tell, this is the first time this question has been answered for a normally quiescent stem cell (hematopoietic stem cells can change their proliferative profile, but at least some are active at all times). The future of regenerative medicine may involve activation of endogenous stem cells. Understanding the proper amount of stem cells to activate is crucial to that goal.

These tools now allow for new types of questions to be answered. One important question is how does the adult regulate its pigment pattern? The drug neocuproine can now ablate melanocytes specifically and only in the adult. While regeneration studies in the larva are constrained temporally by metamorphosis, adult regeneration studies can be done multiple times. Multiple regenerative events can address whether or not the MSC

has a limited regenerative capacity. The adult also has a richer pigment pattern diversity than the larva. While many pigment pattern mutants that affect only the adult pattern (e.g., *rose, leopard, jaguar,* etc.), the mechanisms affecting the MSC to produce these patterns are poorly understood. Challenging these mutants to regenerate as adults can determine if the difference in the pigment pattern of these adults is a reflection in a change in the underlying MSCs, . Mutants that fail to regenerate their pigment pattern would imply that those mutants are defective in the adult MSC. If the first regeneration event is normal, repeated rounds of regeneration could determine if some mutants were defective for MSC maintenance.

Another important question is the relation of the larval zebrafish to the adult. While most of the MSCs in the larvae are employed in a regenerative event, the number of melanocytes in the larvae is an order of magnitude fewer than in the adult (Johnson et al., 1995b). That suggests that during metamorphosis many more MSCs might be recruited to develop the adult pigment pattern. Are these adult MSCs related to the larval MSCs? There is some suggestion that at least some of the adult MSCs are unrelated to the larval MSCs. Chapter 3 predicts that a *kit* homozygote would have no larval MSCs, but the adult does have melanocytes, although not as many as wild type (Johnson et al., 1995b). This question can be addressed using clonal analysis similar to the one Tryon et al. used (2011). After injecting embryonic fish with the lineage vector, these fish can be segregated as larvae based on the presence of regeneration clones and then grown into adults. Screening adults for clones will discover how closely related the MSC in the larvae is related to adult melanocytes. Treating these adult fish with neocuproine, causing regeneration in these adults, can then provide a similar determination of the

relatedness of the metamorphic melanocytes to the underlying MSCs that support the adult pigment pattern.

Additionally, Chapter 3 makes many specific predictions that can be directly tested with a marker for the MSC and/or an early marker for the ontogenetic melanoblast. An MSC marker in wild type should show that during a regenerative event in the larvae that most, but not all MSCs contribute. Additionally, following individual MSCs across 2 sequential regenerative events should reveal several things: nearly all MSCs contribute to at least 1 round; MSCs do not have a refractory period, i.e., they do not need to "rest" between regenerative events; and that many MSCs contribute to both rounds. In the $kit^{null/+}$ mutant, a reduction of the number of MSCs should be observed. With an additional marker for the ontogenetic melanoblast, a transient increase in the number of melanoblasts could be observed in the $kit^{null/+}$ mutant compared to wild type if this marker were expressed early in the lineage. A reduction in early melanoblast symmetric divisions might also be observed in the $kit^{null/+}$ mutant compared to wild type as some of the cells normally fated to become MSCs in the $kit^{null/+}$ mutant are converted into the ontogenetic lineage.

Chapter 3 focuses on lineage analysis, not on direct observation. The ability to directly observe the MSC would allow for different and more complete analysis from Chapter 3. I have shown how often a lineage responds to a regenerative event, but this does not address whether this is the same MSC. Direct observation of the MSC would be conclusive as to whether this was the same MSC or a different, related MSC. This determination is also directly related to the estimates of the number of MSCs in each fish. If instead of 1 MSC, the lineage analysis was performed on 2 closely related MSCs,

my estimates would double. Direct observation of the MSC would allow for trivial quantification of the number of MSCs per fish.

An alternative way to explore whether or not my lineage analysis revealed more than one MSC is through legacy labeling. This would involve labeling the MSC during a first round of regeneration with a legacy marker, such as BrdU or EdU, performing a second round of regeneration without label, and scoring melanocytes for the marker. The only way the marker would be present in melanocytes from the second, unlabeled round of regeneration would be that the MSC producing those melanocytes had incorporated the marker during the first, labeled round of regeneration. That would demonstrate that those MSCs were dividing during both round of regeneration. However, as these markers are not easily incorporated by the fish until 4dpf, this experiment is technically challenging to perform prior to metamorphosis.

The receptor tyrosine kinase *kit* has long been studied in the mouse. However, it can be difficult to study due to the effects it has on several stem cells system. Gene duplication in the zebrafish allows study of *kit* just in the melanocyte lineage, allowing insights into the MSC that are technically challenging to address in the mouse. Despite this difference, melanocyte development has been shown to be highly similar to what occurs in mammals. Thus, my findings regarding the role of *kit* in the establishment of the MSC may not only be applicable to mammals, but work in zebrafish in general may be the best way to evaluate the function of *kit* in the MSC. At the very least, this work can help to guide future work in the mouse MSC.

Chapter 4 provides a guideline for future mutagenesis screens in zebrafish. A primary bottleneck in screens is the time spent on the mutagenesis and screening, so

using mutagenized fish efficiently is or paramount importance. Previous screens, even those done in the lab, may not have been done efficiently in the past. As mutant screens are the first step in discovering new mutants in MSC function, this can aide many future screens in the lab.

REFERENCES

Ashman, L. K. (1999). The biology of stem cell factor and its receptor C-kit. *Int J Biochem Cell Biol* **31**, 1037-51.

Barker, N., van Es, J. H., Kuipers, J., Kujala, P., van den Born, M., Cozijnsen, M., Haegebarth, A., Korving, J., Begthel, H., Peters, P. J. et al. (2007). Identification of stem cells in small intestine and colon by marker gene Lgr5. *Nature* **449**, 1003-7.

Berghmans, S., Murphey, R. D., Wienholds, E., Neuberg, D., Kutok, J. L., Fletcher, C. D., Morris, J. P., Liu, T. X., Schulte-Merker, S., Kanki, J. P. et al. (2005). tp53 mutant zebrafish develop malignant peripheral nerve sheath tumors. *Proc Natl Acad Sci U S A* **102**, 407-12.

Bernstein, J., Patterson, D. N., Wilson, G. M. and Toth, E. A. (2008). Characterization of the essential activities of Saccharomyces cerevisiae Mtr4p, a 3'->5' helicase partner of the nuclear exosome. *J Biol Chem* **283**, 4930-42.

Bowie, M. B., Kent, D. G., Copley, M. R. and Eaves, C. J. (2007). Steel factor responsiveness regulates the high self-renewal phenotype of fetal hematopoietic stem cells. *Blood* **109**, 5043-8.

Budi, E. H., Patterson, L. B. and Parichy, D. M. (2008). Embryonic requirements for ErbB signaling in neural crest development and adult pigment pattern formation. *Development* **135**, 2603-14.

Chakrabati, S., Streisinger, G., Singer, F. and Walker, C. (1983). Frequency of y-ray induced specific locus and recessive lethal mutations in mature germ cells of the zebrafish, Brachydanio rerio. *Genetics* **103**, 109-123.

Chen , S., Lin, J., Liu, S., Liang, Y. and Lin-Shiau, S. (2008). Apoptosis of cultured astrocytes induced by the copper and neocuproine complex through oxidative stress and JNK activation. *Toxicological Science* **102**, 138-49.

Driever, W., Solnica-Krezel, L., Schier, A., Neuhauss, C., Malicki, J., Stemple, C., Stanier, D., Zwartkruis, F., Abdelilah, S., Rangini, Z. et al. (1996). A genetic screen for mutations affecting embryogenesis in zebrafish. *Development* **123**, 37-46.

Gargioli, C. and Slack, J. M. (2004). Cell lineage tracing during Xenopus tail regeneration. *Development* **131**, 2669-79.

Geissler, E. N., Ryan, M. A. and Housman, D. E. (1988). The dominant-white spotting (W) locus of the mouse encodes the c-kit proto-oncogene. *Cell* **55**, 185-92.

Goldsmith, M. I., Iovine, M. K., O'Reilly-Pol, T. and Johnson, S. L. (2006). A developmental transition in growth control during zebrafish caudal fin development. *Dev Biol* **296**, 450-7.

Goodrich, H. and Nichols, R. (1931). The Development and the regeneration of color pattern in brachydanio rerio. *Journal of Morphology* **52**, 512-523.

Gupta, V. and Poss, K. D. (2012). Clonally dominant cardiomyocytes direct heart morphogenesis. *Nature* **484**, 479-84.

Haffter, P., Granato, M., Brand, M., Mullins, M. C., Hammerschmidt, M., Kane, D. A., Odenthal, J., van Eeden, F. J., Jiang, Y. J., Heisenberg, C. P. et al. (1996). The identification of genes with unique and essential functions in the development of the zebrafish, Danio rerio. *Development* **123**, 1-36.

Huang, C. C., Lawson, N. D., Weinstein, B. M. and Johnson, S. L. (2003). reg6 is required for branching morphogenesis during blood vessel regeneration in zebrafish caudal fins. *Dev Biol* **264**, 263-74.

Hultman, K. A., Budi, E. H., Teasley, D. C., Gottlieb, A. Y., Parichy, D. M. and Johnson, S. L. (2009). Defects in ErbB-dependent establishment of adult melanocyte stem cells reveal independent origins for embryonic and regeneration melanocytes. *PLoS Genet* **5**, e1000544.

Hultman, K. A. and Johnson, S. L. (2010). Differential contribution of direct-developing and stem cell-derived melanocytes to the zebrafish larval pigment pattern. *Dev Biol* **337**, 425-31.

Iovine, M. and Johnson, S. L. (2000). Genetic analysis of isometric growth control mechanisms in the zebrafish caudal fin. *Genetics* **155**, 1321-1329.

Jackson, I. J., Chambers, D., Rinchik, E. M. and Bennett, D. C. (1990). Characterization of TRP-1 mRNA levels in dominant and recessive mutations at the mouse brown (b) locus. *Genetics* **126**, 451-9.

Johnson, S. L., Africa, D., Horne, S. and Postlethwait, J. H. (1995a). Half-tetrad analysis in zebrafish: mapping the ros mutation and the centromere of linkage group I. *Genetics* **139**, 1727-35.

Johnson, S. L., Africa, D., Walker, C. and Weston, J. A. (1995b). Genetic control of adult pigment stripe development in zebrafish. *Dev Biol* **167**, 27-33.

Johnson, S. L. and Weston, J. A. (1995). Temperature-sensitive mutations that cause stage-specific defects in Zebrafish fin regeneration. *Genetics* **141**, 1583-95.

Jorgensen, E. and Mango, S. (2002). The art and design of genetic screens: Caenorhabditis elegans. *Nat Rev Genet* **3**, 356-69.

Kawakami, K., Takeda, H., Kawakami, N., Kobayashi, M., Matsuda, N. and Mishina, M. (2004). A transposon-mediated gene trap approach identifies developmentally regulated genes in zebrafish. *Dev Cell* **7**, 133-44.

Koshimizu, U., Sawada, K., Tajima, Y., Watanabe, D. and Nishimune, Y. (1991). White-spotting mutations affect the regenerative differentiation of testicular germ cells: demonstration by experimental cryptorchidism and its surgical reversal. *Biol Reprod* **45**, 642-8.

Kragl, M., Knapp, D., Nacu, E., Khattak, S., Maden, M., Epperlein, H. H. and Tanaka, E. M. (2009). Cells keep a memory of their tissue origin during axolotl limb regeneration. *Nature* **460**, 60-5.

Li, C. L. and Johnson, G. R. (1994). Stem cell factor enhances the survival but not the self-renewal of murine hematopoietic long-term repopulating cells. *Blood* **84**, 408-14.

Livet, J., Weissman, T. A., Kang, H., Draft, R. W., Lu, J., Bennis, R. A., Sanes, J. R. and Lichtman, J. W. (2007). Transgenic strategies for combinatorial expression of fluorescent proteins in the nervous system. *Nature* **450**, 56-62.

Lopes, S. S., Yang, X., Muller, J., Carney, T. J., McAdow, A. R., Rauch, G. J., Jacoby, A. S., Hurst, L. D., Delfino-Machin, M., Haffter, P. et al. (2008). Leukocyte tyrosine kinase functions in pigment cell development. *PLoS Genet* **4**, e1000026.

Luria, S. and Delbrück, M. (1943). Mutations of Bacteria from Virus Sensitivity to Virus Resistance. *Genetics* **28**, 491-511.

Lyons, D. A., Pogoda, H. M., Voas, M. G., Woods, I. G., Diamond, B., Nix, R., Arana, N., Jacobs, J. and Talbot, W. S. (2005). erbb3 and erbb2 are essential for schwann cell migration and myelination in zebrafish. *Curr Biol* **15**, 513-24.

Ma, E. Y., Rubel, E. W. and Raible, D. W. (2008). Notch signaling regulates the extent of hair cell regeneration in the zebrafish lateral line. *J Neurosci* **28**, 2261-73.

Mackenzie, M. A., Jordan, S. A., Budd, P. S. and Jackson, I. J. (1997). Activation of the receptor tyrosine kinase Kit is required for the proliferation of melanoblasts in the mouse embryo. *Dev Biol* **192**, 99-107.

Manova, K. and Bachvarova, R. F. (1991). Expression of c-kit encoded at the W locus of mice in developing embryonic germ cells and presumptive melanoblasts. *Dev Biol* **146**, 312-24.

Martin, G. R. (1981). Isolation of a pluripotent cell line from early mouse embryos cultured in medium conditioned by teratocarcinoma stem cells. *Proc Natl Acad Sci U S A* **78**, 7634-8.

Mellgren, E. M. and Johnson, S. L. (2006). pyewacket, a new zebrafish fin pigment pattern mutant. *Pigment Cell Res* **19**, 232-8.

Mendelsohn, B. A., Yin, C., Johnson, S. L., Wilm, T. P., Solnica-Krezel, L. and Gitlin, J. D. (2006). Atp7a determines a hierarchy of copper metabolism essential for notochord development. *Cell Metab* **4**, 155-62.

Mullins, M. C., Hammerschmidt, M., Haffter, P. and Nusslein-Volhard, C. (1994). Large-scale mutagenesis in the zebrafish: in search of genes controlling development in a vertebrate. *Curr Biol* **4**, 189-202.

Mullins, M. C. and Nusslein-Volhard, C. (1993). Mutational approaches to studying embryonic pattern formation in the zebrafish. *Curr Opin Genet Dev* **3**, 648-54.

Naish, S., Cooksey, C. J. and Riley, P. A. (1988). Initial mushroom tyrosinase-catalysed oxidation product of 4-hydroxyanisole is 4-methoxy-ortho-benzoquinone. *Pigment Cell Res* **1**, 379-81.

Nechiporuk, A., Poss, K. D., Johnson, S. L. and Keating, M. T. (2003). Positional cloning of a temperature-sensitive mutant emmental reveals a role for sly1 during cell proliferation in zebrafish fin regeneration. *Dev Biol* **258**, 291-306.

Nishikawa, S., Kusakabe, M., Yoshinga, K., Ogawa, M., Hayashi, S., Kunisada, T., Era, T., Sakakura, T. and Nishikawa, S. (1991). In utero manipulation of coat color formation by a monoclonal anti-c-kit antibody: two distinct waves of c-kit-dependency during melanocyte development. *EMBO J* **10**, 2111-8.

Nishimura, E. K., Granter, S. R. and Fisher, D. E. (2005). Mechanisms of hair graying: incomplete melanocyte stem cell maintenance in the niche. *Science* **307**, 720-4.

Nishimura, E. K., Jordan, S. A., Oshima, H., Yoshida, H., Moriyama, M., Jackson, I. J., Barrandon, Y., Miyachi, Y. and Nishikawa, S. (2002). Dominant role of the niche in melanocyte stem-cell fate determination. *Nature* **416**, 854-60.

Niu, M. and Twitty, M. (1950). The origins of epidermal melanophores during metamorphosis in trituris torusis. *J Exp Zool* **113**, 633-648.

Osawa, M., Egawa, G., Mak, S. S., Moriyama, M., Freter, R., Yonetani, S., Beermann, F. and Nishikawa, S. (2005). Molecular characterization of melanocyte stem cells in their niche. *Development* **132**, 5589-99.

Oshima, H., Rochat, A., Kedzia, C., Kobayashi, K. and Barrandon, Y. (2001). Morphogenesis and renewal of hair follicles from adult multipotent stem cells. *Cell* **104**, 233-45.

Parichy, D. M., Ransom, D. G., Paw, B., Zon, L. I. and Johnson, S. L. (2000). An orthologue of the kit-related gene fms is required for development of neural crest-derived xanthophores and a subpopulation of adult melanocytes in the zebrafish, Danio rerio. *Development* **127**, 3031-44.

Parichy, D. M., Rawls, J. F., Pratt, S. J., Whitfield, T. T. and Johnson, S. L. (1999). Zebrafish sparse corresponds to an orthologue of c-kit and is required for the morphogenesis of a subpopulation of melanocytes, but is not essential for hematopoiesis or primordial germ cell development. *Development* **126**, 3425-36.

Parichy, D. M. and Turner, J. M. (2003). Zebrafish puma mutant decouples pigment pattern and somatic metamorphosis. *Dev Biol* **256**, 242-57.

Parichy, D. M., Turner, J. M. and Parker, N. B. (2003). Essential role for puma in development of postembryonic neural crest-derived cell lineages in zebrafish. *Dev Biol* **256**, 221-41.

Peterson, R. T., Link, B. A., Dowling, J. E. and Schreiber, S. L. (2000). Small molecule developmental screens reveal the logic and timing of vertebrate development. *Proc Natl Acad Sci U S A* **97**, 12965-9.

Poss, K. D., Nechiporuk, A., Hillam, A. M., Johnson, S. L. and Keating, M. T. (2002). Mps1 defines a proximal blastemal proliferative compartment essential for zebrafish fin regeneration. *Development* **129**, 5141-9.

Quigley, I. K., Turner, J. M., Nuckels, R. J., Manuel, J. L., Budi, E. H., MacDonald, E. L. and Parichy, D. M. (2004). Pigment pattern evolution by differential deployment of neural crest and post-embryonic melanophore lineages in Danio fishes. *Development* **131**, 6053-69.

Raible, D. W., Wood, A., Hodsdon, W., Henion, P. D., Weston, J. A. and Eisen, J. S. (1992). Segregation and early dispersal of neural crest cells in the embryonic zebrafish. *Dev Dyn* **195**, 29-42.

Rawls, J. F., Frieda, M. R., McAdow, A. R., Gross, J. P., Clayton, C. M., Heyen, C. K. and Johnson, S. L. (2003). Coupled mutagenesis screens and genetic mapping in zebrafish. *Genetics* **163**, 997-1009.

Rawls, J. F. and Johnson, S. L. (2000). Zebrafish kit mutation reveals primary and secondary regulation of melanocyte development during fin stripe regeneration. *Development* **127**, 3715-24.

Rawls, J. F. and Johnson, S. L. (2001). Requirements for the kit receptor tyrosine kinase during regeneration of zebrafish fin melanocytes. *Development* **128**, 1943-9.

Rawls, J. F. and Johnson, S. L. (2003). Temporal and molecular separation of the kit receptor tyrosine kinase's roles in zebrafish melanocyte migration and survival. *Dev Biol* **262**, 152-61.

Rinkevich, Y., Lindau, P., Ueno, H., Longaker, M. T. and Weissman, I. L. (2011). Germ-layer and lineage-restricted stem/progenitors regenerate the mouse digit tip. *Nature* **476**, 409-13.

Schultz, E., Gibson, M. C. and Champion, T. (1978). Satellite cells are mitotically quiescent in mature mouse muscle: an EM and radioautographic study. *J Exp Zool* **206**, 451-6.

Sette, C., Dolci, S., Geremia, R. and Rossi, P. (2000). The role of stem cell factor and of alternative c-kit gene products in the establishment, maintenance and function of germ cells. *Int J Dev Biol* **44**, 599-608.

Sheets, L., Ransom, D. G., Mellgren, E. M., Johnson, S. L. and Schnapp, B. J. (2007). Zebrafish melanophilin facilitates melanosome dispersion by regulating dynein. *Curr Biol* **17**, 1721-34.

Snippert, H. J., van der Flier, L. G., Sato, T., van Es, J. H., van den Born, M., Kroon-Veenboer, C., Barker, N., Klein, A. M., van Rheenen, J., Simons, B. D. et al. (2010). Intestinal crypt homeostasis results from neutral competition between symmetrically dividing Lgr5 stem cells. *Cell* **143**, 134-44.

Solnica-Krezel, L., Schier, A. and Driever, W. (1994). Efficient recovery of ENU-induced mutations from the zebrafish germline. *Genetics* **136**, 1401-1420.

Stemple, D. L. and Anderson, D. J. (1992). Isolation of a stem cell for neurons and glia from the mammalian neural crest. *Cell* **71**, 973-85.

Streisinger, G., Singer, F., Walker, C., Knauber, D. and Dower, N. (1986). Segregation analysis and gene-centromere distances in zebrafish *Genetics* **112**, 311-319.

Streisinger, G., Walker, C., Dower, N., Knauber, D. and Singer, F. (1981). Production of clones of homozygous diploid zebra fish (Brachydanio rerio). *Nature* **291**, 293-6.

Sugimoto, M., Uchida, N. and Hatayama, M. (2000). Apoptosis in skin pigment cells of the medaka, Oryzias latipes (Teleostei), during long-term chromatic adaptation: the role of sympathetic innervation. *Cell Tissue Res* **301**, 205-16.

Tegelenbosch, R. A. J. and de Rooij, D. G. (1993). A quantitative study of spermatogonial multiplication and stem cell renewal in the C3H/101 F 1 hybrid mouse. *Mutation Research* **290**, 193-200.

Tryon, R. C., Higdon, C. W. and Johnson, S. L. (2011). Lineage relationship of direct-developing melanocytes and melanocyte stem cells in the zebrafish. *PLoS One* **6**, e21010.

Tsang, S. Y., Tam, S. C., Bremner, I. and Burkitt, M. J. (1996). Research communication copper-1,10-phenanthroline induces internucleosomal DNA fragmentation in HepG2 cells, resulting from direct oxidation by the hydroxyl radical. *Biochem J* **317 (Pt 1)**, 13-6.

Tu, S. and Johnson, S. L. (2010). Clonal analyses reveal roles of organ founding stem cells, melanocyte stem cells and melanoblasts in establishment, growth and regeneration of the adult zebrafish fin. *Development* **137**, 3931-9.

Tu, S. and Johnson, S. L. (2011). Fate restriction in the growing and regenerating zebrafish fin. *Dev Cell* **20**, 725-32.

Valent, P., Spanblochl, E., Sperr, W. R., Sillaber, C., Zsebo, K. M., Aglis, H., Strobl, H., Geissler, K., Bettelheim, P. and Lechner, K. (1992). Induction of differentiation of human

mast cells from bone marrow and peripheral blood mononuclear cells by recombinant human stem cell factor/kit-ligand in long-term culture. *Blood* **80**, 2237-45.

Westerfield, M. (1995). The zebrafish book: a guide for the laboratory use of zebrafish (Danio rerio). Eugene: University of Oregon Press.

Yang, C. T., Hindes, A. E., Hultman, K. A. and Johnson, S. L. (2007). Mutations in gfpt1 and skiv2l2 cause distinct stage-specific defects in larval melanocyte regeneration in zebrafish. *PLoS Genet* **3**, e88.

Yang, C. T. and Johnson, S. L. (2006). Small molecule-induced ablation and subsequent regeneration of larval zebrafish melanocytes. *Development* **133**, 3563-73.

Yang, C. T., Sengelmann, R. D. and Johnson, S. L. (2004). Larval Melanocyte Regeneration Following Laser Ablation in Zebrafish. *Journal of Investigative Dermatology*, 924-929.

Zou, J., Beermann, F., Wang, J., Kawakami, K. and Wei, X. (2006). The Fugu tyrp1 promoter directs specific GFP expression in zebrafish: tools to study the RPE and the neural crest-derived melanophores. *Pigment Cell Res* **19**, 615-27.